



NTNU – Trondheim
Norwegian University of
Science and Technology

Modeling of Hydroelastic Response of Closed Flexible Fish Cages due to Sea Loads

Ida Marlen Strand

Marine Technology

Submission date: July 2013

Supervisor: Asgeir Johan Sørensen, IMT

Co-supervisor: Pål Furset Lader, Sintef Fiskeri og Havbruk
Zsolt Volent, Sintef Fiskeri og Havbruk
Odd Magnus Faltinsen, IMT

Norwegian University of Science and Technology
Department of Marine Technology

MASTER THESIS IN MARINE CYBERNETICS

SPRING 2013

FOR

Ida Strand

Modeling of Hydroelastic Response of Closed Flexible Fish Cages due to Sea Loads

Work description

Closed flexible fish cages are proposed used in the sea, to meet with ecological challenges in the aquaculture industry. Earlier experiences with structural collapse of a similar concept have shown that it is crucial to secure the cage against raptures and escapes. The aim of this thesis is to investigate sea loads on, and response of a Closed Flexible Cage due to current and hydrostatic loads. This work is a continuation of the candidate's previous work. This master thesis should consist of two scientific papers, with a resume.

Scope of work

Resume:

- Describe the Closed Flexible Cage (CFC) concept and the associated operational challenges.
- Review relevant literature related to current loads, hydrostatic pressure forces and subsequent deformations of the CFC.
- Describe and rationalize the methods used for solving the problem of hydrostatic behavior.

Paper one:

- Review and analyze results from the CFC model experiments conducted summer 2012.
- Develop and describe an analytical/empirical model of the forces on a cylindrical shaped bag due to current loads.

Paper two:

- Plan and conduct new CFC model experiments spring of 2013.
- Review and analyze results from the conducted CFC model experiments related to static deformations of the bag, with and without applied passive control with braces.
- Develop and describe an analytical/empirical model of the static deformations on an elliptically shaped bag.
- Propose a method for leakage detection.

The report shall be written in English and edited as an article collection with a resume in front, in the format of a report. It is supposed that the Department of Marine Technology, NTNU,

can use the results freely in its research work, unless otherwise agreed upon, by referring to the student's work. The thesis should be submitted July 21, 2013.

Co-supervisors:

- Dr. Pål Lader, SINTEF Fisheries and Aquaculture
- Dr. Zsolt Volent, SINTEF Fisheries and Aquaculture
- Professor Odd M. Faltinsen, Department of Marine Technology, NTNU

Professor Asgeir J. Sørensen
Supervisor

Abstract

Norway is presently the worlds biggest producer of Atlantic salmon. The traditionally used open-net-structures are probably the most important reason for the Norwegian success. The very nature of aquaculture, where fish is grown at a much higher density than appear naturally, makes it likely to affect the existing surrounding environment. Views on weaknesses related to the traditional technology have been stated. These weaknesses concern sustainability challenges related to escapes, sea-lice, diseases and pollution.

Closed Flexible Fish Cages are proposed used in the sea, to meet with ecological challenges in the aquaculture industry. In a closed fish production system, the farmer has increased control of how the fish are exposed to the environment, by controlling the flow and quality of the water entering and leaving the bag.

A closed flexible floating system is not far from the currently used net cage fish farm systems, and may therefore be easier to put directly into operation. Even though a CFC seems to be an attractive solution, the existing knowledge about how the CFC will respond to external sea loads are limited. More knowledge is needed to understand the response of the cage if this technology are to be utilized in an industrial scale.

Experimental data from towing experiments conducted in the summer of 2012, are analysed to better understand the current forces with connected deformations on the bag for different filling levels. The analysed bag showed an increased tendency to deform for decreasing filling levels, leading to an increase in drag coefficient. A new method for mathematical modelling of the increase in drag, by a filling-level-dependent drag coefficient is proposed.

Earlier experiences with structural collapse of a similar concept have shown that it is crucial to secure the cage against raptures and escapes. To assure this, a method to detect leakage and pump failure at an early stage must be developed. To detect leakages it is important to know how the bag deforms under static conditions for lower filling levels.

Experimental data from experiments conducted in the spring of 2013 was analysed related to deformations on the bag for different filling levels, with and without applied passive control by braces, under static conditions. A new method for modelling the deformed shape of the bag for decreasing filling levels is proposed.

Sammendrag

Norge er i dag verdens største produsent av atlantisk laks. Produksjon av laks i åpne mærder laget av nett, har sannsynligvis vært den viktigste årsaken til den norske suksessen. Konseptet akvakultur, hvor fisk er holdt ved mye høyere tettheter enn det som fremkommer naturlig, vil sannsynligvis påvirke naturen rundt. Bekymringer om bærekraften til den tradisjonelle teknologien har blitt fremmet. Disse bekymringene gjelder spesielt lus, sykdommer og forurensning.

Lukkede fleksible oppdrettsanlegg er foreslått brukt i sjøen som en løsning på de økologiske utfordringene til fiskeriindustrien. I et lukket produksjonssystem for fisk vil røkteren ha økt kontroll på hvordan oppdrettsfisken blir påvirket og påvirker miljøet rundt, ved å kontrollere/ rense vann inn og ut av mærdene.

Et lukket fleksibelt oppdrettsanlegg er ikke langt fra de tradisjonelle nøtene, og kan derfor være enklere å sette direkte i operasjon. Men, på tross av at lukkede fleksible oppdrettsanlegg kan se ut som en attraktiv løsning, er den eksisterende kunnskapen om hvordan dette systemet vil reagere på sjølast, mangelfull. Mer kunnskap er derfor nødvendig for å forstå responsen til det lukkede anlegget før det kan bli brukt i en industriell skala.

Eksperimentelle data fra taue forsøk utført sommeren 2012, er analysert for å forstå hvordan strøm vil påvirke posen ved forskjellige fyllingsgrader. Analysene viser at posen har en økende tendens til å deformere seg, når fyllingsgraden minker. En ny metode for matematisk modellering av økningen i drag, ved bruk av en fyllingsgrad avhengig drag-koeffisient er foreslått.

Tidligere erfaringer med strukturell kollaps av et lignende konsept har vist at det er nødvendig å sikre posen mot rifter og rømmninger. For å sikre dette må det utvikles en metode for å oppdage lekkasjer og pumpefeil på et tidlig stadium. For å oppdage lekkasjer er det viktig å forstå hvordan posen oppfører seg, under statiske forhold, for lave fyllingsgrader.

Eksperimentelle data fra forsøk utført våren 2013 har blitt analysert relatert til deformasjoner på en elliptisk pose for forskjellige fyllingsgrader, med og uten påførte horisontale avstivere, under statiske forhold. En ny metode for modellering av den deformerte formen til en pose ved minkende fyllingsgrad er foreslått.

Preface

This master thesis is written during the spring of 2013 as a part of my studies for the Master of Science degree in Marine Technology at the Norwegian University of Science and Technology (NTNU) in Trondheim.

This work is part of the research project “External Sea Loads and Internal Hydraulics of Closed Flexible Cages” a knowledge-building project for the aquaculture business sector, in cooperation with SINTEF Fisheries and Aquaculture, industry partners and NTNU.

Work related to the second of the appended papers are considered for patent filing, this thesis is therefore until further notice confidential.

Acknowledgements

I am grateful to my supervisor Professor Asgeir Sørensen for his help and advice. His knowledge, enthusiasm and ability to get things done is inspiring. I would also like to thank my co-advisor's Dr. Pål Lader, Dr. Zsolt Volent and Professor Odd Faltinsen for answering questions, helping out in the lab and giving directions.

I would like to thank all the nice guys in the industry group, for being most hospitable, and for sharing their experience and knowledge with me.

A special tanks to my boyfriend Håkon, who fixes all problems.

Ida Strand

Trondheim, 3rd July 2013

Contents

Abstract	v
Sammendrag	vi
Preface	vii
Acknowledgements	viii
1 Introduction	1
1.1 Background and Motivation	1
1.1.1 The Closed Flexible Cage Project	2
1.1.2 Operational Challenges with the CFC	3
1.1.3 The Historic Development of the CFC	4
1.2 Contributions	4
1.3 Organization of Thesis	5
2 Theory	7
2.1 Description of the System	7
2.2 Current Forces and Deformations	8
2.2.1 Current Forces on Rigid Structures	8
2.2.2 Deformation and Current Loads on Bag Pens	10
2.2.3 Current Forces on Net Structures	12
2.3 Hydrostatic Pressure Forces and Deformation Patterns	13
2.3.1 Buoyancy	13
2.3.2 Static Shape of Membrane Structures	14
2.3.3 Shapes of Static Pendant Drops	16
3 Methodology	17
3.1 Problem Description	17
3.2 Possible Research Approaches	17
3.2.1 Conducting Experiments	18
3.2.2 Modelling and Simulation of the System	18

3.2.3	Model Complexity Levels	19
3.3	Research Approach	19
4	Conclusion and Further Work	21
4.1	Conclusion	21
4.2	Recommendations for Further Work	21
	Bibliography	23
A	Appended papers	25
	Paper 1: Modelling of Drag Forces on a Closed Flexible Fish Cage	25
	Paper 2: Modelling and Control of Deformations of Closed Flexible Fish Cages with Leakage Detection	33

List of Figures

1.1	Illustration of a Closed Flexible Cage	2
1.2	Technical description of the bag system used in Flekkefjord	4
2.1	Bag parts, and coordinates system.	7
2.2	Flow regimes circular cylinder	8
2.3	Theoretical and actual pressure distribution on a circular cylinder	9
2.4	Drag coefficient circular cylinder adapted from Blevins (1984)	10
2.5	Drag Coefficient adapted from Blevins (1984)	10
2.6	Deformation of bag pen in current(Rudi and Solaas, 1993).	11
2.7	Pressure distribution and shape of bag in current.	11
2.8	Deformation of net cylinder	12
2.9	A two-dimensional membrane structure. Adopted from (Zhao, 1995)	14
2.10	Description of parameters. Adopted from (Zhao, 1995)	15
2.11	Membrane shape	15
2.12	Shapes of static pendant drops	16

Chapter 1

Introduction

To solve some of the challenges in the aquaculture industry, closed flexible cages are proposed used. The aim of this thesis is to investigate sea loads on, and response of a Closed Flexible Cage due to hydrostatic loads and current.

This thesis consists of two parts. The first part is an introduction with background to the closed flexible cage concept, followed with background theory of current and hydrostatic loads on flexible structures. The second part consists of two papers, one related to current loads on the bag, the other about static deformation of a leak bag. Some of the background and theory are earlier described in (Strand, 2012).

1.1 Background and Motivation

Fish represent a vital contribution to the world's food supply. However, at the same time as the world's population is growing, many marine capture fisheries have become depleted and the fish are harder to catch. The question arises: "Is it possible to meet the increasing demand in seafood?" The only other source for production of fish food is aquaculture (Tidwell and Allan, 2012).

Norway is presently the world's biggest producer of Atlantic salmon. The traditionally used open-net-structures are probably the most important reason for the Norwegian success. The open net-structures is a simple, inexpensive technology that utilises the Norwegian advantage of abundant access to fresh and clean seawater (Rosten et al., 2011).

The very nature of aquaculture, where fish is grown at a much higher density than appear naturally, makes it likely to affect the existing surrounding environment (Crawford and MacLeod, 2009). While the aquaculture facilities have grown in size and number, the attention related to the industry's ecological sustainability have increased. Views on weaknesses related to the traditional technology have been

stated (Rosten et al., 2011). These weaknesses concern sustainability challenges related to escapes, sea-lice, diseases and pollution (Gullestad et al., 2011). See figure 1.1 for illustration.

Presently there are no common, commercially available, technological solution to the described problems. However, if open water closed fish technology can be utilized at an industrial level, it can be used as a possible solution to limit the undesirable environmental impact from farming of salmon (Rosten et al., 2011).

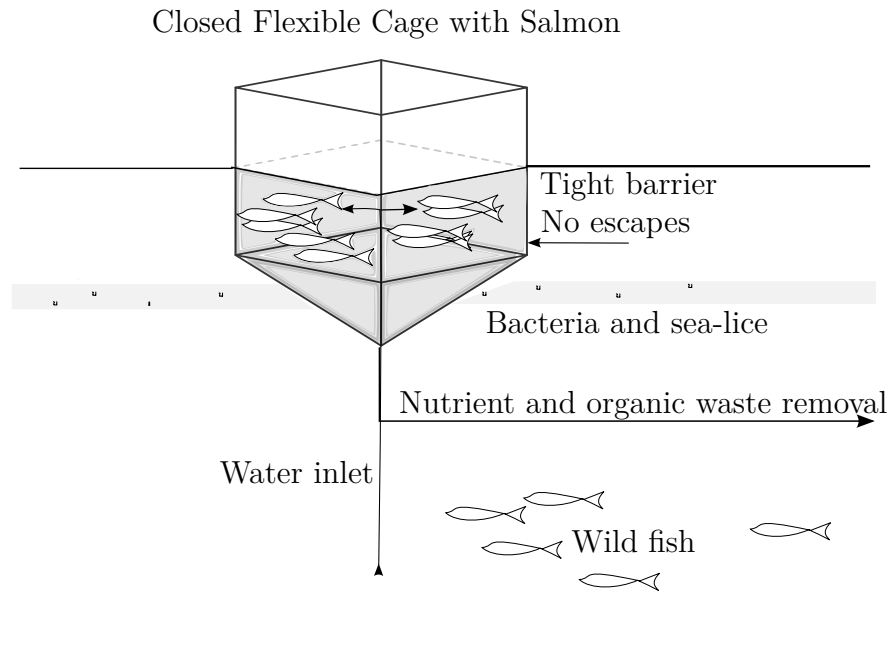


Figure 1.1: Illustration of a Closed Flexible Cage

1.1.1 The Closed Flexible Cage Project

Closed containment technology is a term used to describe technologies that attempt to restrict and control the interaction between the farmed fish and the surrounding environment, with the goal of minimizing the impact and get better control over the aquaculture production (Michael et al., 2010).

In a closed fish production system, the farmer has increased control of how the fish are exposed to the environment, by controlling the flow and quality of the water entering and leaving the bag. By controlling the flow in and out of the bag, it is expected that the waste-pollution will be limited. This causes a more stable environment inside the bag, which can be an advantage related to fish welfare (Rosten et al., 2011).

One way of making a closed fish production system is as a closed flexible cage (CFC). A closed flexible floating system is not far from the currently used net cage fish farm systems, and may therefore be easier to put directly into operation.

Even though a CFC seems to be an attractive solution, the existing knowledge about how the CFC will respond to external sea loads are limited. The hydrodynamic drag forces on the structure are expected to increase compared to a net based structure. The cage is in addition expected to be highly hydro-elastic, meaning that the deformation of the bag is closely coupled to the hydrodynamic forces. The hydrodynamic loads and responses on the CFC are far more difficult to understand, than those of rigid structures.

1.1.2 Operational Challenges with the CFC

The CFC project is expected to be more technologically advanced than the currently used net cages, introducing new operational challenges.

As previously mentioned, is the existing knowledge of the response of the flexible bag limited. Since the forces are expected to increase compared to the net structures, this increase must be kept at a minimum. To lower the forces on the structure, the flexibility of the bag is planned actively used. This can be done if the structure deforms in a favourable way, either passively, or by active control. This can lead to a decrease in drag, either because of a reduced exposed area A , or a reduced drag coefficient C_D . If the system must be controlled to achieve favourable deformations, more knowledge is needed to understand the response of the cage, due to the interdependence of the deformation and the forces on the bag.

The deformation of the cage is expected to affect the water environment inside the cage. To ensure sufficient water quality and flow more knowledge about how and the effect of the deformations of the system is needed.

Water must be exchanged by pumping water in and out, in order to secure a sufficient flow-through. Waste must be removed, as illustrated in figure 1.1. For high densities of fish, the water inside the bag must probably be oxygenated, to limit the maximum capacity of the pumps, as well as keeping the current inside the bag at a acceptable level for the fish to thrive.

Because of the expected, excessive deformations, it is essential to monitor and control the fish environment to make the CFC concept successful. It is also crucial to secure the cage against escapes and structural collapse. If rifts are made in the bag material, the bag can collapse, possibly killing or releasing the fish. To address all these concerns, robust systems, that can cope with the harsh Norwegian environment, must be made.

Design, dimensioning and operation of the CFC will demand increased competence both from the equipment suppliers and the operating personnel (Rosten et al., 2011).

1.1.3 The Historic Development of the CFC

Different versions of the CFC concept have been tested out on several occasions. One of the first Norwegian attempts was at a research-station at Matre, Norway around 1988. The system was then referred to as promising, related to increased growth of salmon during the winter (Rosten et al., 2011).

A similar system was tried out at the start of the nineties, at Støymland Fisk in Flekkefjord also in Norway, as part of a research project run by Agder Research foundation. A test facility was made as illustrated in figure 1.2. The facility was run for four years (Skaar and Bodvin, 1993). The main aim of the project was to

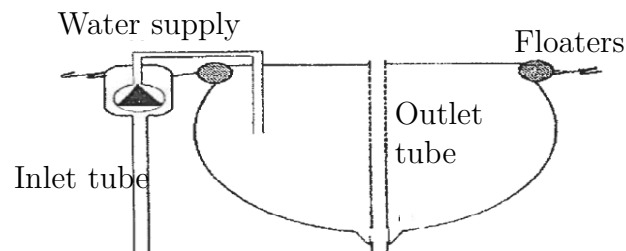


Figure 1.2: Technical description of the bag system used in Flekkefjord, adapted from Skaar and Bodvin (1993)

reduce/control the influence of environmental effects on the fish production. Algae blooms, fish-lice and extreme temperature variations, had been a big problem in this region. A design project was also attached to this project that considered environmental forces on the bag (Rudi and Solaas, 1993).

An upscaled version of the Flekkefjord facility was tried out close to Arendal in 1995. This facility experienced a total breakdown after short time, due to material fatigue, and the concept was abandoned for a time (Rosten et al., 2011).

Today there exists only one test project with a closed bag. This is a EU-research project coordinated by Plast Sveis AS. The project is named Closed Fish Cage. A pilot facility has been tested out in Toft, Brønnøysund from from September 2010 until June 2011. During this time the system has been working without problems, and shown promising results related to sea-lice infestations (Johannessen, 2013).

1.2 Contributions

The following points summarizes the new contributions presented in this thesis:

- Analysis and formulation of drag forces for closed flexible cages with varying filling levels. The contribution is given in the first appended paper: *Modelling of Drag Forces on a Closed Flexible Fish Cage*.

- Analysis and formulation of a model of the static deformations for closed flexible cages with varying filling levels. The contribution is given in the second appended paper: *Modelling and Control of Deformations of Closed Flexible Fish Cages with Leakage Detection*

1.3 Organization of Thesis

Chapter 1 briefly introduce the general background, history and motivation of this thesis.

Chapter 2 presents theory of current forces, hydrostatic pressure forces and connected deformations of flexible and rigid structures.

Chapter 3 presents and discusses possible analysis methods.

Chapter 4 concludes the work, and presents recommendations for further work.

Chapter 2

Theory

Relevant theory for current forces and static pressure forces on the closed flexible cage (CFC) are reviewed .

2.1 Description of the System

The CFC is mainly composed of three parts: A floater, the bag itself and the bag content, see figure 2.1.

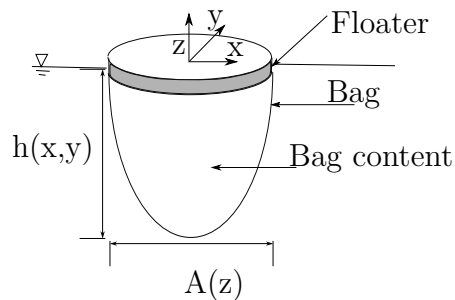


Figure 2.1: Bag parts, and coordinates system.

The bag is flexible and expected to behave in a hydroelastic manner. When a structure is hydroelastic, the forces and deformations of the structure can not be treated separately. The bag will deform to some degree, when subjected to pressure forces. The ability of the bag to deform is expected to increase with decreasing filling level λ , which is given in percent as:

$$\lambda = \frac{V_f}{V_0} 100\% , \quad (2.1)$$

where V_f is the actual amount of water in the bag in litres, and V_0 is the theoretical full filling level.

2.2 Current Forces and Deformations

Current forces on a chosen cylindrical bag geometry, is studied. These current forces are previously described in Strand (2012).

There is sparse direct comparison literature related to drag on flexible, deformable structures available. The only direct comparison source found for the CFC was the conference paper by Rudi and Solaas (1993), which described pressure distribution and bag deformation caused by current on a bag pen.

Because of the lack of literature, related work was applied. Three different comparison cases are applied to cover the forces and deformation of the bag.

2.2.1 Current Forces on Rigid Structures

When subjected to current forces a membrane structure will after a transient period have adapted to a steady state form. This form can be compared to that of a rigid structure, than known models for drag can be applied.

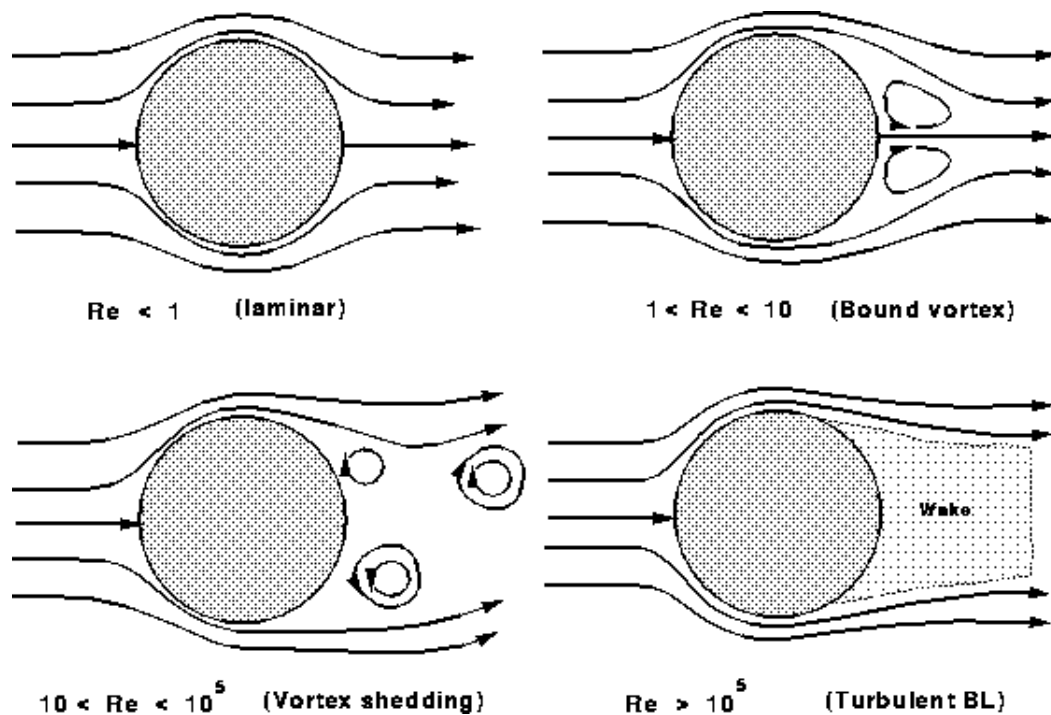


Figure 2.2: Flow regimes circular cylinder, adapted from White (2003)

Drag refers to forces which act on a solid object in the direction of the relative fluid flow velocity. The extent of drag depends on the different flow regimes (laminar to turbulent) influencing the structure. Due to the difficulties modelling the flow

separation behind the structure, the theory is esteemed weak. Because of this a semi-empirical approach is used, by applying a drag coefficient. The drag force on a structure in a uniform flow can be expressed as:

$$F_D = \frac{1}{2}\rho U^2 A C_D \quad (2.2)$$

where ρ is the fluid density, V is the free stream velocity, A is the projected frontal area, and C_D is a dimensionless drag coefficient.

Drag is composed of two parts. One part due to pressure differences between the high pressure points in the front and low pressures in the separated region behind, called pressure drag. The pressure drag is dependent of the flow regime the cylinder is under as illustrated in figure 2.2.

The pressure drag on a rigid circular cylinder is presented in figure 2.3 for both theoretical and experimentally found turbulent and laminar flow.

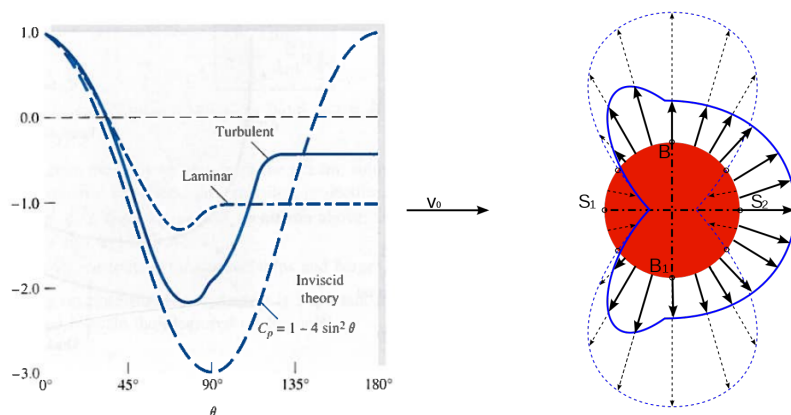


Figure 2.3: Theoretical and actual pressure distribution on a circular cylinder adapted from White (2003), θ is the angle of the cylinder from 0 to 180 clockwise.

The second drag contribution is from shear stress or friction drag on the body. Both parts give contributions to the drag coefficient.

$$C_D = C_{D, \text{pressure}} + C_{D, \text{friction}}$$

Dimensional analysis shows that C_D is dependent of the subsection shape, Reynolds number $Re = UD/\nu$, angle of attack Θ between the body and the flow, surface roughness ϵ and Mach number M (Blevins, 1984).

$$C_D = F(\text{shape}, Re, \Theta, \epsilon/D, M)$$

Drag Coefficient, Rigid Circular Cylinder

Our cylinder bag can be approximated, when the bottom part is neglected, as a rigid 3D cylinder.

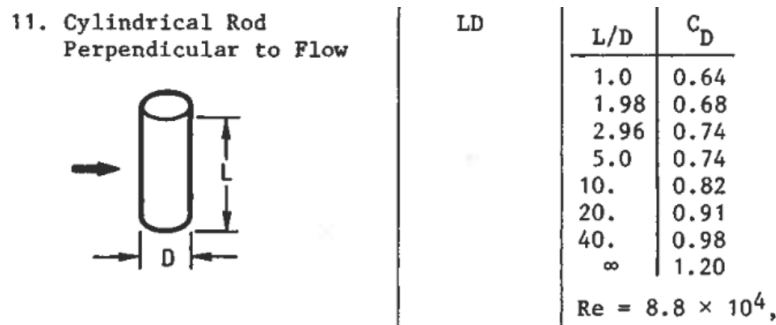


Figure 2.4: Drag coefficient circular cylinder adapted from Blevins (1984)

Conferring figure 2.4 we see that the theoretical drag coefficient closest to our experimental relation L/D , is $L/D = 1$ where $C_D = 0.64$.

Drag Coefficient on a Rigid Hemispherical Cup

A hemispherical cup was observed forming on the front of the bag (facing the current), when the filling level was below full, $\lambda < 100\%$. The drag coefficient for a thin hemispherical cup is described in Blevins (1984), as shown in figure 2.5.

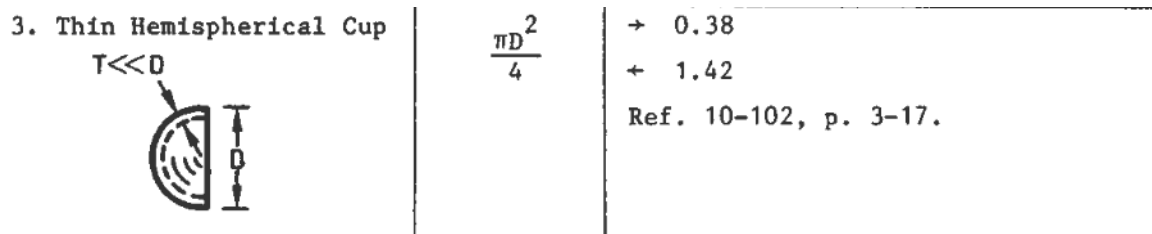


Figure 2.5: Drag Coefficient adapted from Blevins (1984)

2.2.2 Deformation and Current Loads on Bag Pens

Rudi and Solaas (1993) modelled the environmental forces on a bag pen, which is an early type of the CFC. Global current forces were modelled and a drag coefficient C_D of 0.7 was used of practical reasons. The deformation of the bag because of the current was estimated.


$$\alpha = \arctan\left(\frac{1}{2} \frac{F_C}{\Delta p D^2/4}\right)$$


Figure 2.6: Deformation of bag pen in current(Rudi and Solaas, 1993).

The vertical deformation of the bag pen due to current was approximated based on moment equilibrium. The magnitude of the deformation angle α depended on the current force F_C and the pressure difference at the bottom of the bag Δp . It was assumed that the deformation of the bag would be equal on the front and back side as shown in figure 2.6.

Local deformations of the bag wall was assumed originating from the varying pressure distribution around the bag in current. This pressure distribution was estimated using a rigid circular cylinder in steady flow.

The over/under pressure Δz_c was found as

$$\Delta z_c = \frac{C_p U^2}{2g}$$

where C_p is the pressure coefficient of the current velocity, and g is the gravity constant.

Negative Δz_c express overpressure, whereas positive Δz_c express underpressure inside the bag. Δz_c applied on a cylindrical shape is illustrated in figure 2.7. It can be observed from the figure that the bag will be pressed inwards in an area of two times 30° upstream (Rudi and Solaas, 1993).

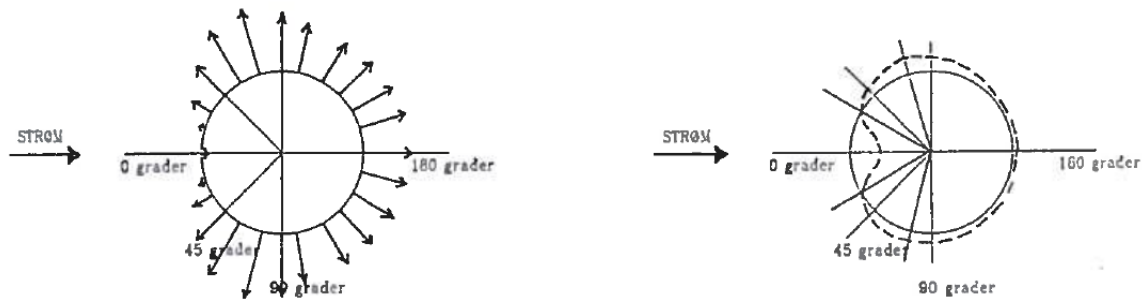


Figure 2.7: Pressure distribution and shape of bag in 1 m/s current. The deflection is magnified for illustration purpose, courtesy of Rudi and Solaas (1993)

2.2.3 Current Forces on Net Structures

The CFC can be compared to the another flexible hydroelastic structure, the net sea cage.

When exposed to current, a net cage change form. The extent of the change depends on the current velocity, and how the net is constructed. Exposed to a uniform current the resulting forces on the net can be divided into two parts: one lift force and one drag force. Both the drag and the lift forces are proportional to AV^2 (Lader et al., 2008).

For net structures it is found that when exposed to current the net deforms at both the front and the back wall, as can be seen in figure 2.8. This is because the net is permeable and the current flows trough the net. When both the front and back wall is deformed the bottom lifts, reducing the exposed area of the cylinder and in turn lowering the forces on the net (Lader and Enerhaug, 2005).

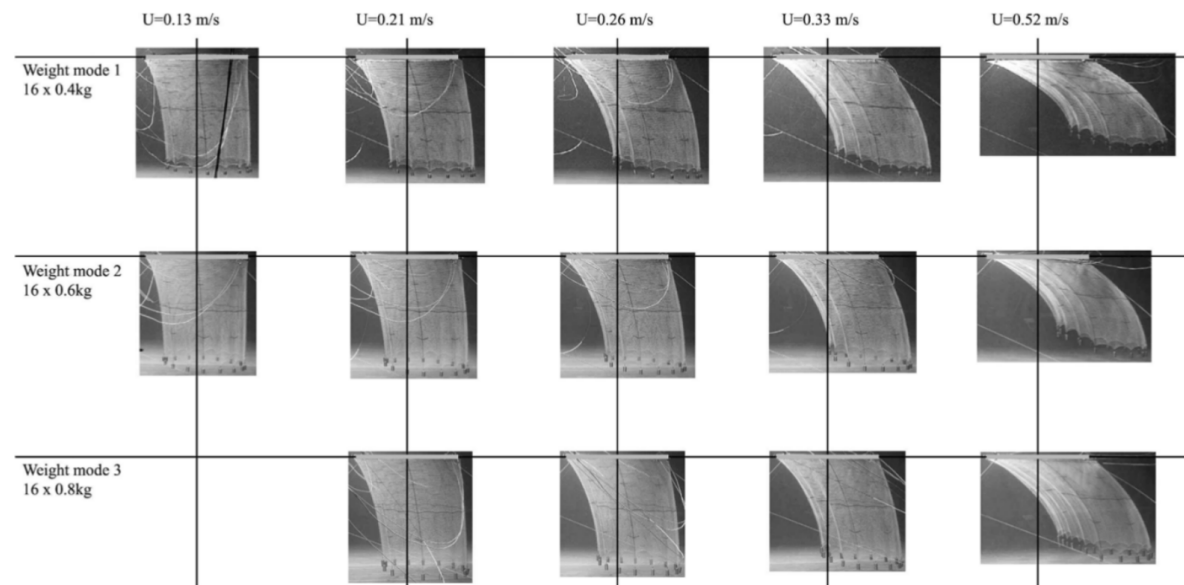


Figure 2.8: Deformation of net cylinder for different weight configurations and current velocities adapted from Lader and Enerhaug (2005)

2.3 Hydrostatic Pressure Forces and Deformation Patterns

Deformation patterns of a partly filled bag, due to static pressure forces is studied.

No literature is found describing the deformations due to hydrostatic pressure of partly filled, open, floating, flexible bags. Therefore, comparison literature for related cases are also applied here. First buoyancy on rigid and flexible structures are presented, before static shapes of membrane structures are described. At last shapes of static pendant drops is considered.

2.3.1 Buoyancy

Archimedes discovered the laws of buoyancy in the third century b.c, where the law for floating objects are given as:

A floating body displaces its own weight in the fluid which it floats.

This law gives the relation:

$$g \times \text{displaced mass} = \text{Floating body weight},$$

$$g\rho \int_A h(x, y)dA = gM, \quad (2.3)$$

where g is the gravity, ρ_w is the density of the water, $h(x, y)$ is the draft of the body and M is the mass of the body (White, 2003).

For a boat the buoyancy results in that the draft of the vessel changes with the weight of the ship. However, for a flexible structure floating at the surface, containing liquid, as our bag, it would be expected that the body would deform to obey this relation.

The majority of the floating body weight of the CFC is origination from the enclosed liquid inside the bag. When the filling level is considered, (2.3) becomes:

$$g\rho_c \frac{\lambda}{100} V_f = g\rho_w \int_A h(x, y)dA, \quad (2.4)$$

where ρ_c is the density of the content of the bag. The floater of the cage is fixed to the free surface, so for decreasing λ , the bag most deform to comply with (2.4), since both the exposed area dA and the draft of the body can deform, this renders multiple shapes for the same volume possible.

2.3.2 Static Shape of Membrane Structures

The CFC can be classified as a liquid filled, membrane structure, another liquid filled membrane structure is the “Dracone” barge, first described by (Hawthorne, 1961). The Dracone barge is a long and flexible liquid-filled tube used for transportation of liquid with density lighter than the surrounding water, such as alcohol, oil or fresh water.

Zhao (1995) described the static shape and stresses of a membrane tube in calm water, they found that the hydroelastic deformations of the cross subsection was highly dependent of the filling level.

A typical cross subsection of a tube in calm water is shown in figure 2.9. The fluid densities inside and outside the tube are ρ_i and ρ_o , and that $\rho_o > \rho_i$. The membrane structure is very thin, and flexible with almost zero bending stiffness, the mass of the membrane itself is therefore ignored.

The static shape of the membrane was given by the following equation:

$$\frac{d\theta}{ds} = \frac{\Delta P}{T}, \quad (2.5)$$

where θ and s is defined in figure 2.10, ΔP is the difference in static pressure inside and outside the membrane and T is the static hoop tension.

The static shape of a two dimensional tube was assumed symmetric about the vertical axis. For a given point a_s and pressure P_{in}^0 , see figure 2.10, only one convex shape was found. It was assumed that the angle θ was equal to π at both the top at a_s and at the bottom at b_e . The problem was then solved numerically, by the shooting method.

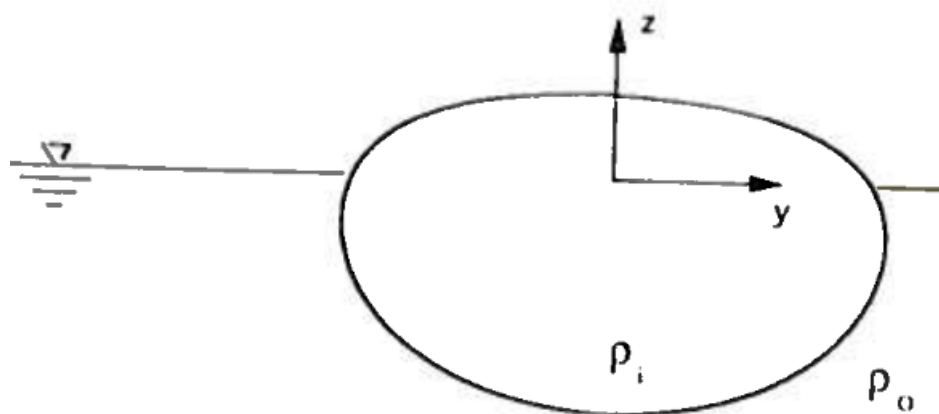


Figure 2.9: A two-dimensional membrane structure. Adopted from (Zhao, 1995)

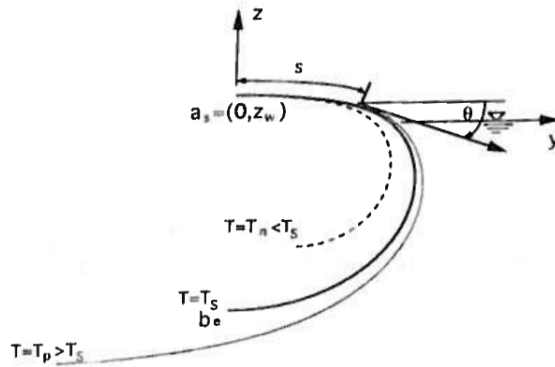


Figure 2.10: Description of parameters. Adopted from (Zhao, 1995)

The static shapes for different filling ratios are presented in figure 2.11, for different filling ratios and relative densities ρ_i/ρ_o . The differences due to differences in density were observed to be small. Meaning that the hydro elastic deformations of the tube were mainly dependent on the filling ratio.

This theory is not applicable when the static hoop tension T drops below zero. Theoretically it is possible with negative tension in membranes, but membranes have negligible compression stiffness, and will when subjected to negative tension buckle, and wrinkles will appear (Shaw and Roy, 2007).

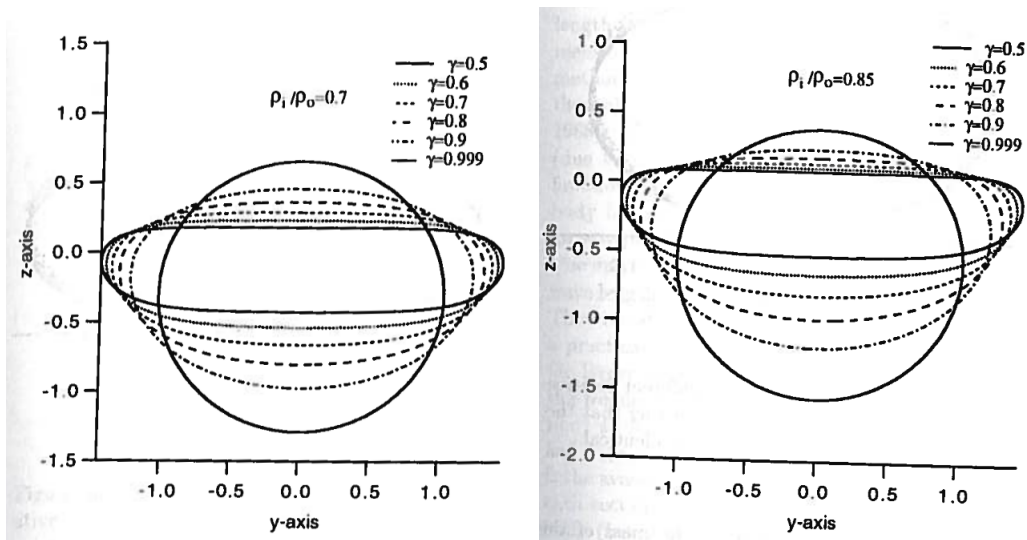


Figure 2.11: Membrane shape, dependent on filling level and relative density ρ_i/ρ_o . Adopted from (Zhao, 1995).

2.3.3 Shapes of Static Pendant Drops

Theoretically the CFC can display multiple deformation patterns for the same filling level, another object displaying the same is the static pendant drop. Two-dimensional and axisymmetric drops hanging under gravity from a solid surface have been studied analytical and numerically in Sumesh and Govindarajan (2010). It was here found that axisymmetric drops can display multiple solutions for the same volume, however some of these shapes were found to be non-physical and not found in the nature.

A liquid drop hanging from a horizontal solid surface, subjected to gravity and surface forces are considered. The shapes of the drops are obtained by variational principles. For a given volume, the shape where the energy is at an optimum is obtained. This is shown in figure 2.12.

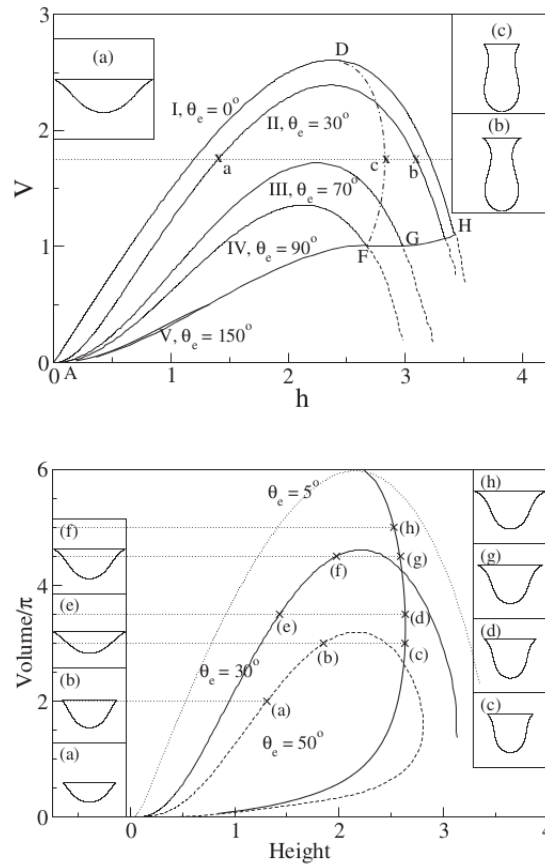


Figure 2.12: Top: Shape and volume of extreme energy shapes as a function of height for 2D drops. Bottom: Typical shapes of antisymmetric drops. Adopted from (Sumesh and Govindarajan, 2010).

Chapter 3

Methodology

To better understand how the Closed Flexible Cage responds to sea loads, increased knowledge is necessary. This chapter presents the methods chosen to analyse the described problems and the rationale behind the choice of method.

3.1 Problem Description

The effects of current forces and hydrostatic pressure on a floating CFC in the form of a membrane bag in water with density ρ_w , containing a liquid with density ρ_c are studied.

As described in section 2.1, is the cage hydroelastic, meaning that the forces on the bag and the structural response can not be treated separately, rendering time domain analysis of the coupling necessary. As also described in section 2.1 is the deformations of the bag expected to increase for decreasing filling levels. Due to the coupling of the forces and deformations, are knowledge about the behaviour of both the forces and the deformations for decreasing filling level, and the relationship between them, important for better understanding of how the cage behaves.

3.2 Possible Research Approaches

To collect the data that is needed, the most effective and appropriate method must be utilized. Which method is best suited highly depends on the problem at hand (Walliman, 2011).

To gain knowledge about the behaviour of the cage, two approaches are suitable, conducting model experiments on the bag, or mathematically modelling and simulating the behaviour of the bag.

3.2.1 Conducting Experiments

Data can be collected by conducting model experiments. The experiment aim to isolate an event without disturbances from its surroundings. Data are generated when you isolate and manipulate one or more variable, and observe the effect of this manipulation (Walliman, 2011).

In order to be able to generalize the results from the model experiments it is important that the experiment possesses both internal and external validity. Internal validity meaning that the experiment actually measures what it is meant to, and external validity means that the findings can be generalized to other settings, the behaviour of the system must be scalable (Walliman, 2011). Both internal and external validity can be compromised by faulty measures and errors in the experiments.

To perform reliable model tests, two aspects are important, namely the physical modelling and the measurement technique (Løland and Aarsnes, 1994).

The most important scaling requirement for an elastic model is:

- *Geometric similarity*
- *Elastic similarity*

Due to practical considerations Froude scaling must to be used for the geometric similarity. This implies that the Froude number $Fr = U/\sqrt{gL}$, must be equal in model and full scale, giving the scale $\Lambda = L_P/L_M$, where subscripts M and P indicate model and full scale respectively. Using the first requirement, the second requirement result in that

$$(Et)_M = (Et)_P/\Lambda^2, \quad (3.1)$$

where Et is the elasticity of the fabric (Løland and Aarsnes, 1994).

3.2.2 Modelling and Simulation of the System

The purpose of a model is to provide a representation of a system, that shows the relationship between variables, this is done by isolating and simplifying an event (Walliman, 2011). As with experiments it is essential to understand the system to be modelled. Identifying the most important variables, and the relation between them.

It is common practice to compare the results from a model to experimental data, or full scale measurements of the problem in question.

Typical modelling tools used for simulating marine systems are numeric solvers of mathematical models such as: the Finite Element Methods (FEM) and Computational Fluid Dynamics (CFD). For some limited problems, analytical solutions have been developed.

3.2.3 Model Complexity Levels

When modelling a system, awareness of the needed complexity level is important. Sørensen (2011) described two complexity levels in mathematical modelling of dynamic systems:

- A *Control plant model* is a simplified description containing only the main physical properties of the system.
- A *Process plant model* is a comprehensive description of the actual system and should be as close to the natural process as possible. The main purpose of this model is to simulate the real physics.

3.3 Research Approach

The coupling between structural response and forces complicates numerical simulations, and demands a challenging time domain analysis. Hydroelastic analysis have previously been conducted with both FEM and CFD, however as we are expecting large deformations, moving boundaries, and both an internal and an external flow problem, a numerical simulation is expected to be mathematically challenging and computationally demanding. For later validation of such a model it is important to build up a solid basis of insight of the physical system by experiments.

To gain more insight into the physical system, model experiments are conducted. This to build a basis for understanding a complex structure.

Based on the model experiments, control plant models are developed. The development of a process plant model of the bag, possibly based on numerical tools, must be left for further study.

Experimental set-up given for the planned and executed experiments are given in the appended papers. The experiments were conducted in two sessions for validation.

Chapter 4

Conclusion and Further Work

4.1 Conclusion

The present thesis focus on the response of a Closed Flexible Cage due to current and hydrostatic loads. To study this experiments have been conducted, and analysed. Simple control plant models have been developed.

The main conclusions of the appended papers are summarized as follows:

- Drag forces on a Closed Flexible Cage for different filling levels was experimentally studied, and a significant increase in drag was experienced as the filling level decreased. This drag increase was found to be due to a large deformation of the front wall facing the current, leading to a significant increase in the drag coefficient. A filling level dependent drag coefficient model was proposed.
- Static deformations of a elliptical CFC for different filling levels was experimentally studied. The image material showed a clear tendency that the bag deforms under static pressure when the bag is less than 100% full. These deformations increase in magnitude, with decreasing filling level. Multiple deformation patterns were found, dependent on filling level and previously applied load. For the braced bag only one deformation pattern was found. A model for a filling-level-dependent deformed draft was presented, and a method for leakage detection have been proposed.

4.2 Recommendations for Further Work

During the course of this work, several interesting and important problems that need further study have been identified. The following issues are recommended for further study:

- Analyse the resulting data from the experiments conducted the spring of 2013 related to current and waves.
- Investigate how the shape and relative dimensions (diameter/draft) of an elliptic cage influence the forces and deformations.
- Investigate how the conducted experiments relate to planned full scale experiments.
- Develop a numerical model of the Closed Flexible Cage, to use as a process plant model. Possibly by finite element modelling (FEM).

Bibliography

- R. D. Blevins. *Applied fluid dynamics handbook*. Van Nostrand, New York, 1984.
- C. Crawford and C. MacLeod. Predicting and assessing the environmental impact of aquaculture. In *New technologies in aquaculture*. CRC, 2009.
- P. Gullestad, S. Bjørgo, I. Eithun, A. Ervik, R. Gudding, H. Hansen, R. Johansen, M. Osland, A. and Rødseth, I. Røsvik, H. Sandersen, and H. Skarra. Effektiv og bærekraftig arealbruk i havbruksnæringen. Technical report, Rapport fra et ekspertutvalg oppnevnt av Fiskeri- og kystdepartementet, 2011.
- W. Hawthorne. The early development of the dracone flexible barge. In *Proceedings of the Institution of Mechanical Engineers 1847-1982*, 1961.
- T. Johannessen. Closedfishcage, June 2013. URL <http://www.closedfishcage.com/>.
- P. Lader and B. Enerhaug. Experimental investigation of forces and geometry of a net cage in uniform flow. *Oceanic Engineering, IEEE Journal of*, 30(1), jan 2005.
- P. Lader, T. Dempster, A. Fredheim, and Ø. Jensen. Current induced net deformations in full-scale sea-cages for atlantic salmon (*salmo salar*). *Aquacultural Engineering*, 38(1), 2008.
- G. Løland and J. Aarsnes. Fabric as construction material for marine applications. In *Hydroelasticity in marine technology*, pages 275 – 286, 1994.
- E. Michael, P. Chadwick, G. J. Parsons, and B. Sayavong. Evaluation of closed-containment technologies. In *Evaluation of Closed-Containment Technologies for Saltwater Salmon Aquaculture*. NRC REsearch Press, 2010.
- T. Rosten, Y. Ulgenes, K. Henriksen, and U. Winther. Oppdrett av laks i lukkede anlegg:forprosjekt. Technical report, SINTEF Fiskeri og havbruk, Trondheim, 2011.

- H. Rudi and F. Solaas. Floating fish farms with bag pens. In *International Conference on Fish Farming Technology*, 1993.
- A. Shaw and D. Roy. Improved procedures for static and dynamic analyses of wrinkled membranes. *Journal of Applied Mechanics*, 74(3):590–594, 2007.
- A. Skaar and T. Bodvin. Fullscale production of salmon in floating enclosed systems. In *International Conference on Fish Farming Technology*, 1993.
- A. J. Sørensen. *Marine control systems : propulsion and motion control of ships and ocean structures*. Trondheim : Marinteknisk senter, Institutt for marin teknikk, 2011.
- I. Strand. Project thesis marine cybernetics. modelling of current forces on closed flexible cages. Technical report, NTNU, 2012.
- P. Sumesh and R. Govindarajan. The possible equilibrium shapes of static pendant drops. *Journal of Chemical Physics*, 133(14), 2010.
- J. Tidwell and G. Allan. The role of aquaculture. In *Aquaculture Production Systems*. Wiley-Blackwell, 2012.
- N. Walliman. *Research methods : the basics*. London : Routledge, 2011.
- F. White. *Fluid Mechanics*. WCB/McGraw-Hill, 2003.
- R. Zhao. A complete linear theory for a two-dimensional floating and liquid-filled membrane structure in waves. *Journal of Fluids and Structures*, 9(8), 1995.

Appendix A

Appended papers

Paper 1

"Modelling of Drag Forces on a Closed Flexible Fish Cage"

Ida Marlen Strand, Asgeir J. Sørensen, Pål Lader and Zsolt Volent

Submitted for the *9th IFAC Conference on Control Applications in Marine Systems (CAMS2013)*. Osaka, Japan.

Modelling of Drag Forces on a Closed Flexible Fish Cage

Ida Marlen Strand* Asgeir J. Sørensen* Pål Lader**
Zsolt Volent**

* *Centre for Autonomous Marine Operations and Systems (AMOS)*
Department of Marine Technology
Norwegian University of Science and Technology, NTNU
NO-7491 Trondheim, Norway
** *SINTEF Fisheries and Aquaculture*
NO-7465 Trondheim, Norway

Abstract: To cope with ecological challenges in the aquaculture industry, Closed Flexible Fish Cages (CFC) are proposed used in the sea. However, the existing knowledge about how the CFC will respond to external sea loads are limited. More knowledge is needed to understand the response of the cage if this technology are to be utilized in an industrial scale. In this paper a new method for mathematical modelling of the increase in drag, for decreasing filling level of a closed flexible cage is proposed. A model for a filling-level-dependent drag coefficient is presented. Experimental data are analysed related to forces and deformations on the bag for different filling levels. The analysed bag showed an increased tendency to deform for decreasing filling levels, leading to an increase in drag coefficient.

Keywords: Aquaculture, drag, hydro-elastic

1. INTRODUCTION

By use of open net structures in the sea, Norway have become the worlds biggest producer of Atlantic salmon. However while the aquaculture facilities have grown in size and number, the industry challenges related to escapes, sea-lice, diseases and pollution have increased (Rosten et al., 2013).

One possible solution to the aquaculture industry challenges is to make a closed floating fish production system in the sea. In a closed system, the control of flow and quality of the water entering and leaving the bag is possible. One way of making a closed fish production system is as a Closed Flexible Cage (CFC). A CFC is not far from the currently used net cage systems, and may therefore be easier to put directly into operation.

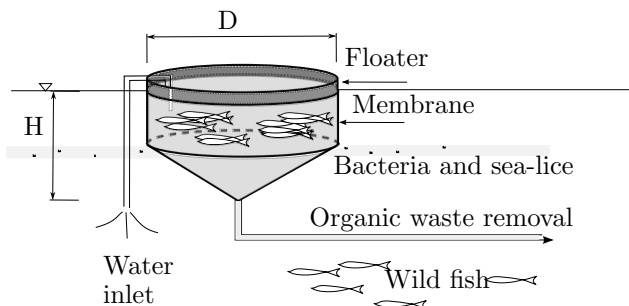


Figure 1. Closed Flexible Cage with salmon.

The CFC is made of a membrane material, in the form as a cylindrical bag with a cone at the bottom as illustrated in figure 1.

The existing knowledge about how a CFC will respond to external sea loads is limited. The hydrodynamic drag forces on the structure are expected to increase compared to a net based structure. The bag is flexible and expected to behave hydro-elastically, meaning that the deformation of, and hydrodynamic forces on the bag are closely coupled. Due to the hydroelasticity of the structure, the hydrodynamic loads and responses of the CFC are expected to be more complex, than those of rigid structures (Rosten et al., 2013). The ability of the bag to deform is expected to increase with decreasing filling level λ , which is given in percent as:

$$\lambda = \frac{V_f}{V_0} \cdot 100\% , \quad (1)$$

where V_f is the actual amount of water in the bag in litres, and V_0 is the theoretical full filling level.

It is crucial to secure the cage against escapes and structural collapse, therefore the forces on the bag must be at a minimum. To limit the forces on the structure, the flexibility of the bag is planned actively used, by controlling the filling level of the bag. The forces will decrease if the structure deforms in a favourable way, either passively, or by active control of the shape. To control the cage with needed stability and performance more knowledge is needed to understand the response.

The object of this paper is to investigate drag forces on, and the response of a Closed Flexible Cage, from analysis of experimental data making a simplified mathematical model of how the loads, deformation and resulting response are dependent on the internal filling level of the bag.

The main contribution of the paper is the analysis and formulation of drag forces for closed flexible cages with varying filling levels.

2. CURRENT FORCES AND DEFORMATIONS

The drag force on a structure in uniform flow can be expressed as:

$$F_D = \frac{1}{2} \rho A C_D V_c^2, \quad (2)$$

where ρ is the fluid density equal to 1000 kg/m^3 for fresh water, V_c is the current velocity, A is the projected frontal area and C_D is a dimensionless drag coefficient. C_D is dependent of the shape of the body and the flow regime around the body. The Reynolds number, given as $Re = \frac{VD}{\nu}$ is used as a non-dimensional measure of the characteristics of the flow regime, where D is a characteristic length of the body, here the diameter, and ν is the kinematic viscosity of the fluid, for fresh water $\nu = 1 \cdot 10^{-6}$. The flow is typically turbulent for high velocities, large Re and laminar for very low velocities, low Re .

If a membrane structure after a transient period adapt to a stationary form, this form can be compared to the form of a rigid structure. Theoretical models for drag for the deformed shape of the body for a rigid structures may then be applied. The CFC can be approximated, when the bottom part is neglected, as a rigid 3D cylinder. Blevins (1984) gives the theoretical drag coefficient closest to our H/D relation as $C_{De} = 0.64$.

Rudi and Solaas (1993) modelled the environmental forces on a bag pen, which is an early type of the CFC. Global current forces were modelled and hydroelastic deformations of the bag due were estimated.

The global vertical deformation of the bag pen was approximated based on moment equilibrium, the deformations are shown in figure 2(b). Local deformations of the bag

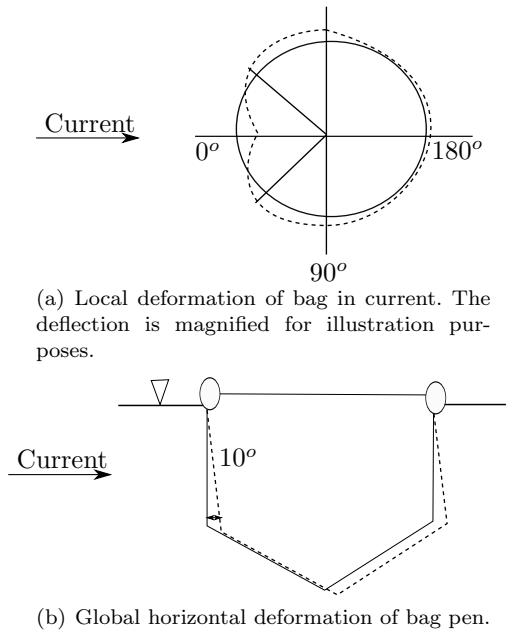


Figure 2. Deformations of a bag pen in current, adapted from Rudi and Solaas (1993).

wall were assumed originating from the varying pressure distribution around the bag in current. This pressure distribution was estimated using a rigid circular cylinder in steady flow as a basis. The local deformations are shown in figure 2(a). Due to the pressure variations the bag was pressed inwards in an area of two times 30 deg upstream, drawing the contour of a hemispherical cup deformation.

The drag coefficient for a thin hemispherical cup is given in Blevins (1984) as $C_{De} = 1.42$.

3. EXPERIMENTAL SETUP

To better understand how current loads affect the CFC for different filling levels and current velocities, model experiments were conducted. The model experiments took place in the small towing tank at US Naval Academy in Annapolis from June 30th to August 17th 2012.

The model was made of a nylon parachute material, in scale 1:50, with dimensions as shown in table 1.

Table 1. Full scale and model scale dimensions

	Diameter	Height cylinder	Height cone
Full scale	38.20 [m]	15.00 [m]	15.00 [m]
Model scale	0.76 [m]	0.30 [m]	0.30 [m]

The model was rigidly attached to a circular bagholder as shown in figure 3. The bag holder was connected to the carriage.

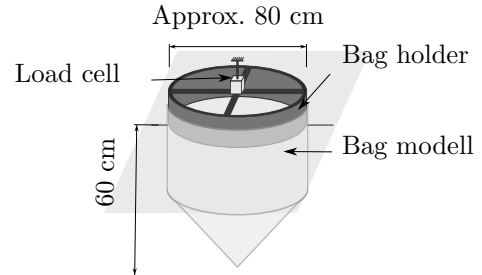


Figure 3. Attachments

Vertical and horizontal forces were measured with a load cell. Drag forces were found by taking the average of the measurement time series over 30 seconds of the horizontal forces for each run. To get the best measurements and steady state velocity, the carriage was run for at least 15 seconds before time averaging started.

Table 2. Full scale current (V_c) and model towing velocities (V_m) with connected Reynolds numbers

Full scale		Model scale	
V_c [m/s]	Re [-]	V_m [m/s]	Re [-]
0.15	$5 \cdot 10^6$	0.021	$1 \cdot 10^4$
0.20	$7 \cdot 10^6$	0.028	$2 \cdot 10^4$
0.30	$10 \cdot 10^6$	0.042	$3 \cdot 10^4$
0.40	$13 \cdot 10^6$	0.057	$4 \cdot 10^4$
0.50	$16 \cdot 10^6$	0.071	$5 \cdot 10^4$
0.60	$20 \cdot 10^6$	0.085	$6 \cdot 10^4$
0.70	$23 \cdot 10^6$	0.099	$6 \cdot 10^4$
0.80	$26 \cdot 10^6$	0.113	$7 \cdot 10^4$
0.90	$29 \cdot 10^6$	0.127	$8 \cdot 10^4$

Nine different current velocities were tested by towing the carriage. The quality (accuracy) of the carriage speed were poor for speeds below 0.02 m/s, limiting the possible minimum current. Full scale and model scale velocities with connected Reynolds number are found in table 2.

For model scale velocities we see from table 2 that Re is in the area of $Re \approx 10^4$, which is the subcritical flow regime, giving a laminar boundary layer. For the full scale current velocities we are around the supercritical and the transcritical flow regime, giving a turbulent boundary layer (Faltinsen, 1990). The change from subcritical to transcritical flow regime will affect C_D , for an undeformed circular cylinder. However, the bag is expected to deform for decreasing filling levels, introducing changes in the bag geometry. If sharp corners are introduced, Blevins (1984) states that the drag coefficient is independent of Re for $Re > 10^4$, making the drag coefficient scalable.

To test the influence of different filling levels on the forces and deformation of the bag, the bag were subjected to four different filling levels λ . The filling levels were:

$$100\%, \quad 90\%, \quad 80\%, \quad 70\% .$$

To measure/observe the deformations of the bag, a system of four cameras were put up as shown in figure 4.

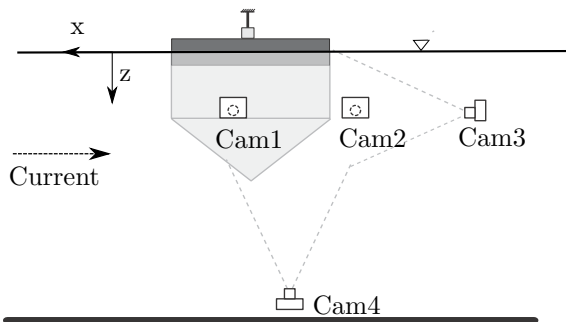


Figure 4. Side view of camera location

Pictures were taken of the structure from three different angles to capture the deformations of the bag. To avoid disturbing the incoming current, no camera was placed in front of the bag.

To estimate the exposed area of the bag, coordinates of the images from the third camera were translated to real world coordinates by a image calibration, using known coordinates in calibration pictures. Coordinates of the edges of the geometry were found, placed as illustrated in figure 5. The top cylinder formed exposed area were approximated as two trapezoids and the cone bottom as a triangle. The estimated error of the placement of the coordinates are in the order of ± 5 cm.

The exposed area A was found according to:

$$\begin{aligned} A_1 &= \frac{1}{4}(y_2 - y_1 + y_4 - y_3)(z_3 - z_1 + z_4 - z_2), \\ A_2 &= \frac{1}{4}(y_4 - y_3 + y_6 - y_5)(z_5 - z_3 + z_6 - z_4), \\ A_3 &= \frac{1}{2}(y_6 - y_5)\left(z_7 - \frac{z_5 + z_6}{2}\right), \\ A &= A_1 + A_2 + A_3. \end{aligned} \quad (3)$$

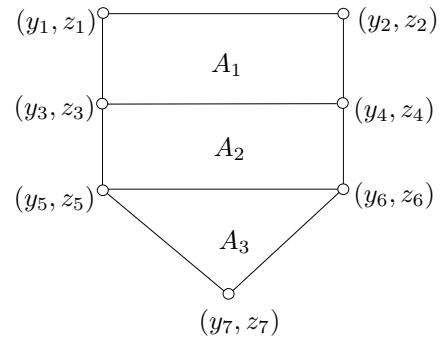


Figure 5. Illustration of placement of coordinates used for area calculation

4. EXPERIMENTAL RESULTS

4.1 Drag force

Measured drag force for all filling levels were plotted and compared to (2) in figure 6.

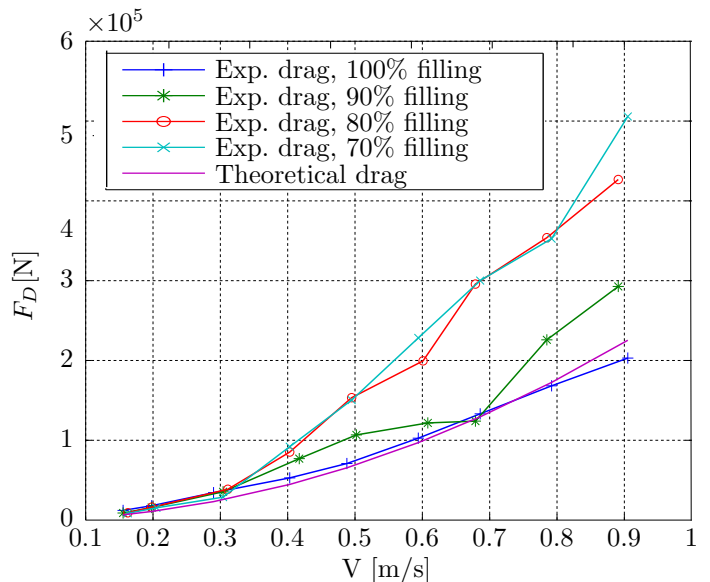


Figure 6. Drag force on the bag for different filling levels as a function of current velocity

Looking at figure 6 we see that the drag forces on the structure increases with decreasing λ . Equation (2) with constant area A and the drag coefficient of a circular cylinder $C_{Dc} = 0.64$ is accurate for the 100% filling level. However as the filling level decreases, (2) underpredicts to an increasing extent, the drag forces on the bag.

Relating the increase in drag for decreasing filling levels to (2), three main hypothesis may be suggested:

- (1) The projected exposed area A of the structure increases as the filling level decreases.
- (2) As the filling level decreases, the body deforms causing the drag coefficient C_D to increase.
- (3) A combination of the former.

The hypothesis were examined successively.

4.2 Exposed area

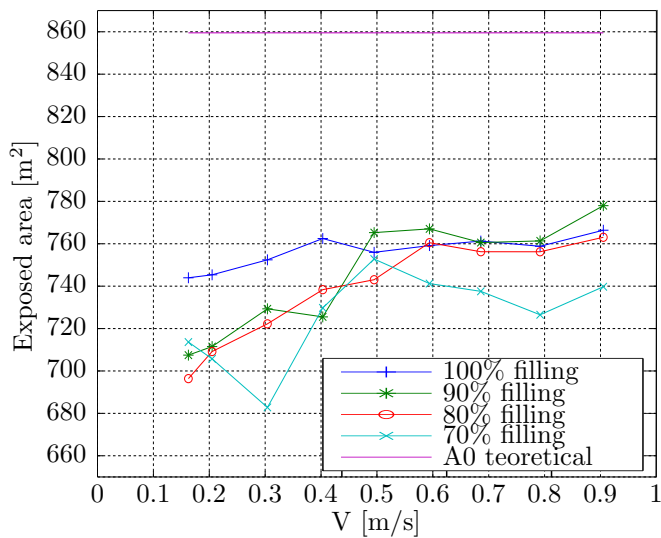


Figure 7. Full scale measured exposed area of bag.

From measurements of exposed area A shown in figure 7, no significant increase in the exposed area was observed, for decreasing filling levels. The measurements of the 70% filling level area indicates the opposite, a decrease in exposed area.

All the measured areas were smaller than the theoretical exposed area A_0 . The under prediction of the exposed areas by the measurements related to A_0 is assumed mostly due to distortion in the images.

Due to the nature of the measurement technique and calculations of the area estimates, an uncertainty of approximately $\pm 10\%$ is assumed.

Despite the errors in the measurement technique, the data indicate that there is no significant increase in exposed area for decreasing filling level.

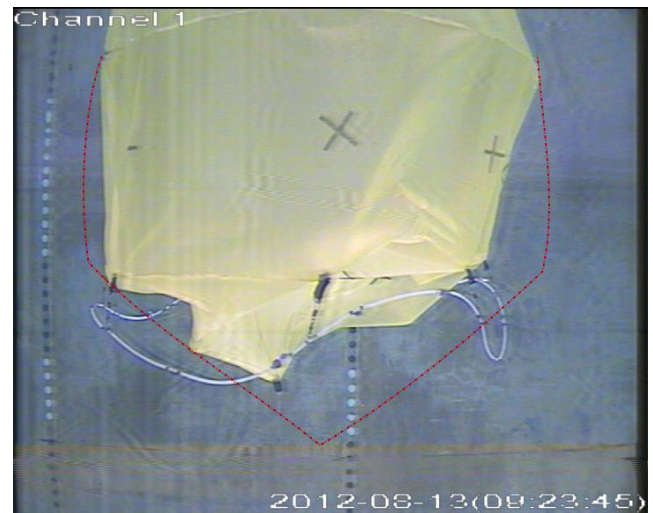
4.3 Deformations

Qualitative analysis of the images from the experiment were done to see if the body showed signs of deformations that could effect the drag coefficient C_D .

The image material showed a clear tendency that the body deformed when the bag was less than 100% full. These deformations increased with decreasing filling level.

For $V_c \leq 0.3$ m/s the body did not appear much affected by the current as shown in figure 8(a), the deformations show only small changes related to the deformed form as it appear for only static pressure.

As for $V_c > 0.3$ m/s the bag displayed similar deformation of the front wall as described in Rudi and Solaas (1993), shown in figure 2(a). When the bag was exposed to current, a hemispherical cup was seen forming at the front. The deformation increased in size for decreasing filling levels. The deformation is shown for the 70% filling level in figure 8(b), and the hemispherical cup is indicated with the black dotted line. For the 70% filling level the bottom was



(a) Deformation pattern for 70% filled cylindrical bag, for $V_c \leq 0.3$ m/s. Undeformed borders for 100% full bag at 0 m/s indicated in red.



(b) Deformation pattern for 70% filled cylindrical bag, for $V_c > 0.3$ m/s. Undeformed borders for 100% full bag at 0 m/s indicated in red. The hemispherical cup deformation is indicated with a dotted black line.

Figure 8. Deformation patterns for 70% filled bag.

observed to be deformed, this could explain the decrease in measured area for this filling level.

The back and sides perpendicular to the current were not observed to deform, even for low filling levels and high current velocities, as can be seen in figure 8(b), where the back wall of the bag follows the borders of the undeformed bag. No deformation of the back wall is contrary to the global current deformations described by Rudi and Solaas (1993) and shown in figure 2(b). The reason for the lack of global deformation is most probably that the local deformation patterns become so pronounced.

It was observed that the bag had an increasing tendency to deform for increasing velocities and decreasing filling levels, it is plausible that the observed deformations could effect C_D .

4.4 Drag coefficient

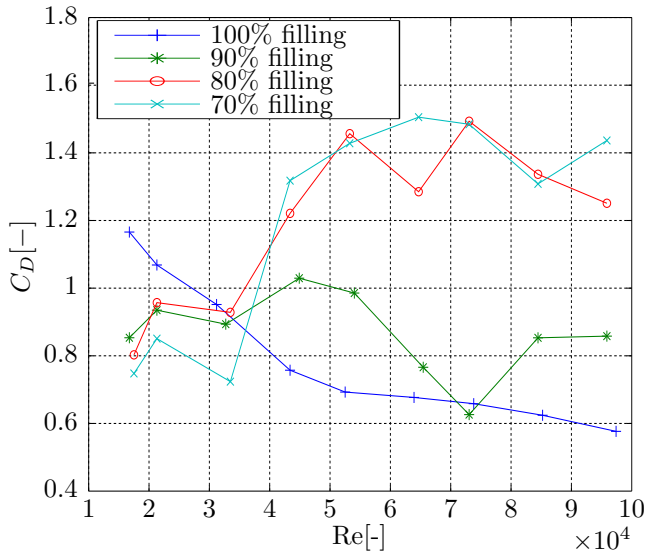


Figure 9. Model scale drag coefficient C_D as a function of Reynolds number Re .

C_D was found from the drag force measurements with constant area A_0 according to:

$$C_D = \frac{F_D}{\frac{1}{2}\rho A_0 V_c^2}. \quad (4)$$

C_D for model scale were plotted against Reynolds number in figure 9 for all the filling levels.

Figure 9 indicates a significant increase in drag coefficient for $Re \leq 4 \cdot 10^4$. This is consistent with the deformation patterns observed in section 4.3. For $Re > 4 \cdot 10^4$ the bag is unaffected by the current, it appear almost static, while for $Re \leq 4 \cdot 10^4$ the characteristic hemispherical cup have appeared.

Mean drag coefficients $\overline{C_D}(\lambda)$ are calculated for the different filling levels for $Re \leq 4 \cdot 10^4$, according to:

$$\overline{C_D}(\lambda) = \frac{1}{6} \cdot \sum_{i=3}^9 C_D(\lambda)_i. \quad (5)$$

The resulting $\overline{C_D}(\lambda)$ are given in table 3.

Table 3. Mean experimental drag coefficient

λ [%]	100	90	80	70
$\overline{C_D}(\lambda)$ [-]	0.66	0.85	1.34	1.41

From table 3 it is observed that the drag coefficient for 100% filling, $\overline{C_D}(100)$ is not far from the drag coefficient of the circular cylinder $C_{Dc} = 0.64$, while when the bag is 70% full, $\overline{C_D}(70)$ indicates that C_D proceeds towards the drag coefficient of the hemispherical cup $C_{De} = 1.42$.

For decreasing λ the body deforms to a such extent that it is expected that the flow behind the body is fully turbulent. C_D for $\lambda < 100\%$ is therefore expected to be valid for full-scale.

5. MODELLING OF FILLING LEVEL DEPENDENT DRAG COEFFICIENT

From the model experiments on the closed flexible cage a large increase in drag force on the bag was experienced for $\lambda < 100\%$. Analysis of the exposed area, deformations and drag coefficient on the bag clearly indicates that the increase in drag is caused by an increase in drag coefficient originating from a deformation of the bag. Since the passive deformations of the cage were unfavourable active control of the form of the cage is probably needed to keep the forces at a minimum. However to be able to control the cage, it is crucial to understand the response of the uncontrolled cage. To estimate the correct drag forces, a model for the drag coefficients dependency of the filling level is needed.

$\overline{C_D}(\lambda)$ was used as a basis for modelling the filling level dependent drag coefficient $C_D(\lambda)$. Based on table 3, the data indicates that $\overline{C_D}(100\%) \approx C_{Dc} = 0.64$ and will for decreasing filling level, down to $\lambda \leq 70\%$ increase to $\overline{C_D}(70\%) \approx C_{De} = 1.42$, see figure 10.

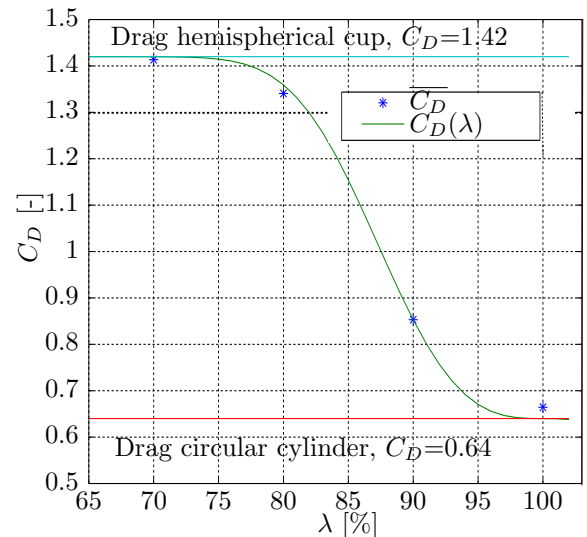


Figure 10. Drag coefficient model

A simple relation is proposed for the transition from $C_{Dc} \rightarrow C_{De}$:

$$C_D(\lambda) = C_{De} + (C_{Dc} - C_{De}) \cdot e^{c(1-\lambda)^n} = 1.42 - 0.78e^{c(1-\lambda)^n}, \quad (6)$$

where n is a real integer, describing the form of the function, and c is an unknown coefficient found from fitting of the equation to the experimental data.

c is found by solving (6) for a known filling level λ_k and an experimentally known drag coefficient $\overline{C_D}(\lambda_k)$, and n is found by minimizing the error ϵ between the model and $\overline{C_D}$ for $1 \leq n \leq 4$.

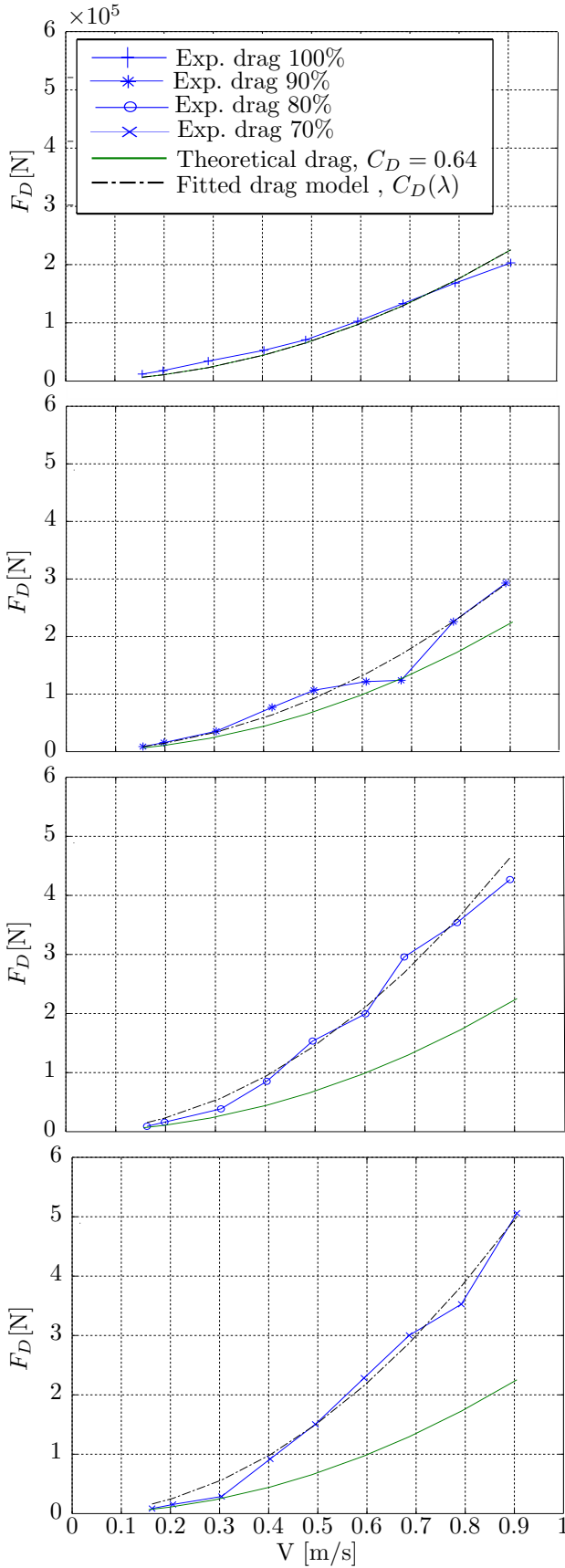


Figure 11. Drag forces on the bag for 100% , 90% , 80% and 70% filling as a function of current velocity. Experimental results plotted together with the theoretical model with constant drag coefficient $C_D = 0.64$ and fitted drag model $C_D(\lambda)$.

Using $\lambda_k = 90\%$ and $\overline{C_D}(90\%) = 0.85$, yields:

$$c = \frac{\ln\left(1 - \frac{\overline{C_D}(\lambda_k) - C_{Dc}}{C_{De} - C_{Dc}}\right)}{(1 - \lambda_k)^n},$$

$$= -\frac{0.313}{0.1^n}, \quad (7)$$

$$\epsilon_n = \sum_{i=1}^4 |\overline{C_D}(\lambda_i) - C_D(\lambda_i)_n|. \quad (8)$$

The resulting c and ϵ_n for $1 \leq n \leq 4$, are given in table 4.

Table 4. c values for given n , cylinder

n	1	2	3	4
c	-3.14	-31.36	-313.66	-3136.58
ϵ_n	0.65	0.20	0.05	0.11

The least error is found for $n = 3$. By applying $n = 3$ and the associated c , the resulting model yields:

$$C_D(\lambda) = 1.42 - 0.78 \cdot e^{-313.66(1-\lambda)^3} \quad (9)$$

Equation (9) is used in (4) and compared to the experimental results, and (4) with a constant $C_D = C_{Dc}$ in figure 11. From figure 11 it is now seen that (9) with $C_D(\lambda)$ predicts the increase in drag on the bag for decreasing λ .

6. CONCLUSION

To utilize Closed Flexible Cage technology at an industrial level more knowledge is needed to understand the sea loads on the structure. Drag forces on a Closed Flexible Cage for different filling levels have been experimentally studied, and a significant increase in drag was experienced as the filling level decreased. This drag increase was found to be due to a large deformation of the front wall facing the current, leading to a significant increase in the drag coefficient. A filling level dependent drag coefficient model have been proposed.

7. ACKNOWLEDGEMENTS

This work have been financed by the industry project "External Sea Loads and Internal Hydraulics of Closed Flexible Cages" a knowledge-building project for the aquaculture business sector, in cooperation with SINTEF Fisheries and Aquaculture and NTNU, and the Norwegian Research Council.

The authors would also like to thank the professional and technical staff at the U.S. Naval Academy Hydromechanics Laboratory for their support.

REFERENCES

- R. D. Blevins. *Applied fluid dynamics handbook*. Van Nostrand, New York, 1984.
- O.M Faltinsen. *Sea Loads on ships and offshore structures*. Cambridge University Press, 1990.
- T Rosten, B. F. Terjesen, Y. Ulgenes, K. Henriksen, E. Biering, and U. Winther. Lukkede oppdrettsanlegg i sjø- økt kunnskap er nødvendig. *Vann*, (1), 2013.
- H. Rudi and F Solaas. Floating fish farms with bag pens. In *International Conference on Fish Farming Technology*, 1993.

Paper 2
**"Modelling and Control of
Deformations of Closed Flexible
Fish Cages with Leakage
Detection"**

Ida Marlen Strand, Asgeir J. Sørensen and Zsolt Volent

Unpublished.

Modelling and Control of Deformations of Closed Flexible Fish Cages with Leakage Detection

Ida Marlen Strand* Asgeir J. Sørensen* Zsolt Volent**

* *Centre for Autonomous Marine Operations and Systems (AMOS)*

Department of Marine Technology

Norwegian University of Science and Technology, NTNU

NO-7491 Trondheim, Norway

** *SINTEF Fisheries and Aquaculture*

NO-7465 Trondheim, Norway

Abstract: Closed Flexible Fish Cages are proposed used in the sea, to meet with ecological challenges in the aquaculture industry. Earlier experiences with structural collapse of a similar concept have shown that it is crucial to secure the cage against raptures and escapes. To assure this a method to detect leakage and pump failure at an early stage must be developed. To detect leakages it is important to know how the bag deforms under static conditions for lower filling levels. In this paper a new method for modelling the deformed shape of the bag for decreasing filling level is proposed. Experimental data are analysed related to deformations on the bag for different filling levels, under static conditions.

Keywords: Aquaculture, static deformations, hydro-elastic

1. INTRODUCTION

While Norway have become the worlds biggest producer of Atlantic salmon, the attention given to the industry challenges related to escapes, sea-lice, diseases and pollution have increased (Rosten et al., 2013). Due to this challenges, a considerable pressure is put on the salmon aquaculture industry to introduce technologies and practices that reduce the influence from the aquaculture on the environment.

A possible solution to the aquaculture industry's challenges is to make a closed floating fish production system in the sea, with the goal of restricting and controlling the interaction between the fish farm and the surrounding environment. One way of making such a system is as a Closed Flexible Cage (CFC). A CFC is not far from the currently used net cage systems, and may therefore be easier to put directly into operation. The CFC described in this paper is made of a membrane material, in the shape of an ellipsoid, as shown in figure 1.

A concept similar to the CFC was tested out at the start of the 1990's, and the project reached commercial full scale tests, but was terminated due to a full structural collapse of one the bags. An episode with collapse due to pump shut-down also occurred (Rosten et al., 2013). This shows that it is crucial to secure the cage against structural collapse and escapes. To assure this, a method to detect leakage and pump failure at an early stage must be developed.

To detect leakages, it is important to know how the bag deforms under static conditions for lower filling levels, as a mean to understand how the bag will behave when it leaks.

If the bag deforms in a consistent favourable way, either autonomous or by passive control with applied braces, the knowledge of the deformations can be used to crate a method for leakage detection.

The object of this paper is to investigate and describe the deformations of the bag under static conditions for different filling levels, with and without applied passive control by horizontal braces, and to develop a system for early leakage detection. From analysis of experimental data a simplified mathematical model of deformation patterns dependent on the filling level is made, and this model is used to estimate the deformed draft of the bag.

The scientific main contribution of this paper is the analysis and formulation of a model of the static deformations for closed flexible cages with varying filling levels.

Organisation of paper: In Section 2, background theory of static deformations are presented. Section 3 contains description of the experimental set-up. The experimental results are analysed in Section 4, and a simplified model of the deformations are presented in Section 5. Finally, conclusions are given in Section 6.

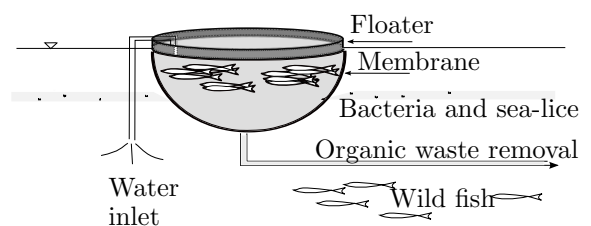


Figure 1. Closed Flexible Cage with salmon.

2. STATIC PRESSURE DEFORMATIONS

The flexibility of a fabric structure is governed by the elasticity of the material and the tension in the fabric. When a flexible structure is exposed to external loads, the response is a change in shape. Due to this response it is no longer possible to decouple the hydrodynamic and the structural analysis, and the problem must be treated hydro-elastically (Løland and Aarsnes, 1994).

The bag is flexible and is expected to deform when subjected to external forces, as shown for current in Strand et al. (2013). For the static case the bag is expected to deform until the system reaches an equilibrium. How the bag deforms can be dependent on several parameters:

- Filling level.
- Mass distribution of the bag material, if weights are attached to the cloth.
- Stiffness of the bag material and possible stiffeners.
- Tension in the fabric.
- Density differences between the content of the bag and the surrounding water.
- Load history effects.

Løland and Aarsnes (1994) have shown that the shape and tension are strongly dependent on the filling level. The tension decreases with decreasing filling level. Theoretically it is possible with negative tension in membranes, but membranes have negligible compression stiffness, and will when subjected to negative tension buckle, and wrinkles will appear (Shaw and Roy, 2007).

2.1 Description of the system

The CFC will mainly be composed of three parts: A floater, the bag itself and the bag content, see figure 2.

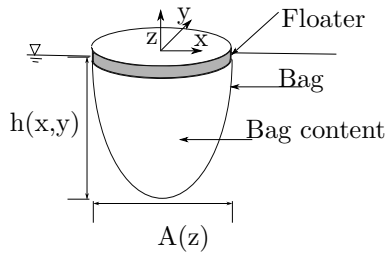


Figure 2. Bag parts, and coordinates system.

The global force contributions from the different parts are described in figure 3.

The vertical force equilibrium when the form has settled become:

$$F_{b_f} - F_{g_f} - F_{g_c} + T_{\theta} - F_{g_B} + F_{h_s} = 0.$$

$$\rho g A_f h_f - g(m_f + \rho_c \nabla + m_B) + T_{\theta} + \rho g \int_A h(x, y) dA = 0.$$

where b denotes buoyancy, g gravity, f floater, c content and B bag. A_f , h_f and m_f is the area, draft and mass of the floater, $\rho_c \nabla$ is the mass of the content inside the bag and $\rho g \int_A h(x, y) dA$ is the static pressure force on the bag. For this case, the mass of the bag material m_b is constant over the whole area.

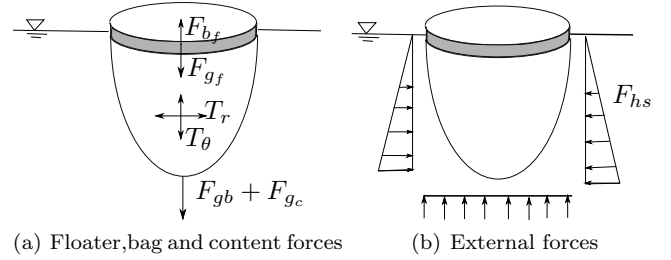


Figure 3. External and internal forces on the bag. Where subscript f denotes floater, b denotes bag and c denotes content.

The ability of the bag to deform is expected to increase with decreasing filling level λ , which is given in percent as:

$$\lambda = \frac{V_f}{V_0} \cdot 100\% , \quad (1)$$

where V_f is the actual amount of water in the bag in litres, and V_0 is the filling level when the bag membrane appear without wrinkles, and is filled with water.

As the filling level decreases, the deformations increase, such that the resulting loads and responses of the bag will in general not longer be linear.

For lower than 100% filling levels, it is observed that wrinkles form under static conditions, this indicate that the tension $T_{\theta} \leq 0$, therefore T_{θ} will be neglected. The buoyancy of the floater F_{b_f} , the gravity forces on the floater F_{g_f} and the gravity forces on the bag itself, F_{g_b} will be small compared to the gravity forces of the content of the bag F_{g_c} , and will therefore also be neglected. The resulting equation becomes:

$$-\rho g \nabla + \rho_c g \int_A h(x, y) dA = 0, \quad (2)$$

where ∇ is the given volume contained inside the bag, and $h(x, y)$ is the hydrostatic draft of the bag. When $\rho_c = \rho$, the equation reduces to the geometric relation:

$$\nabla = \int_A h(x, y) dA. \quad (3)$$

If $\nabla = \lambda V_0$, then for a given $\lambda \leq 100\%$ the equation indicates that there exist multiple deformation patterns, for the same volume. Multiple shapes for the same volume is also found for a similar problem; static pendant drops. It is found that many shapes are theoretically possible for the same volume, but only few of these are stable in the nature (Sumesh and Govindarajan, 2010). Considering (3), with symmetric deformations, three different possible deformation patterns should exist:

- (1) The hydrostatic draft $h(x, y)$ reduces, either by lifting the bottom, or wrinkling the bag sides upwards.
- (2) The exposed area $A(z)$ reduces, by contraction of the sides.
- (3) A combination of the former

3. EXPERIMENTAL SETUP

To better understand the static deformations of the bag, model experiments were conducted. The model experiments took place at the Marine Cybernetics Laboratory at NTNU, Tyholt in two successive rounds. The first from 4.-9. March and the second from 6.-11. May 2013.

The model was made in an elliptic shape of a nylon parachute material, in scale 1:17, with dimensions as shown in table 1.

Table 1. Full scale and model scale dimensions

	Diameter, D	Draft, h
Model scale	0.75 m	0.58 m
Full scale	12.75 m	9.86 m

The bag was attached to a floater in the water surface. To avoid ovalization during towing the floater was stiffened by ropes in the horizontal water plane. Drag forces were measured in the towing direction by load cells. Under the wave experiments springs were added between the bag and the load cell, to allow the bag to follow the wave better. Model and measurement set-up is shown in figure 4.

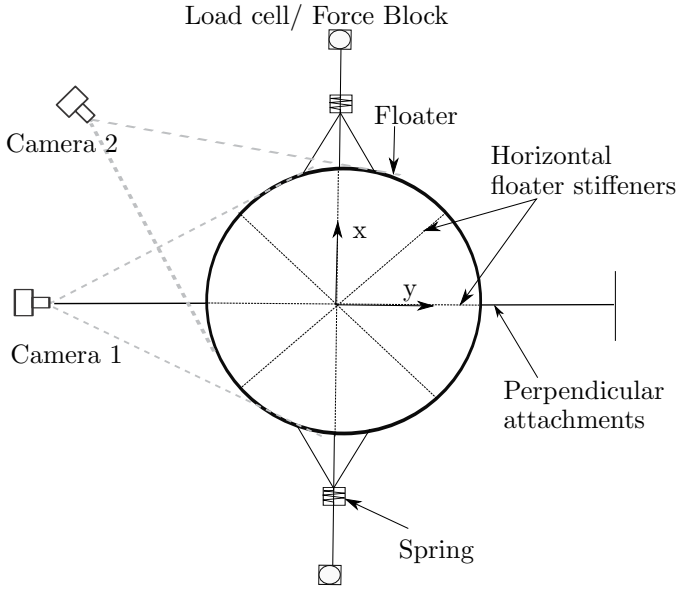


Figure 4. Experimental set-up of load cells, floater and camera positions.

To test the influence of different filling levels on the forces and deformation of the bag, the bag were subjected to five different filling levels λ . The 100% filling level was found by observing when the walls of the bag did not have any wrinkles and appeared smooth, but before the floater sunk. The filling levels are given in table 2.

Table 2. Filling levels of the bag

Filling level	100 %	90 %	80 %	70 %	60 %
Volume	180 l	162 l	144 l	126 l	108 l

The amount of water filled into and emptied out of the bag was measured for control.

To measure/observe the deformations of the bag, videos were taken of the structure from two different angles, under all the different experiments. Two cameras were attached to the carriage as shown to the left in figure 4.

The bag was tested in two configurations. First the bag was tested without any further modifications, then the bag was braced in sections horizontally downwards with stiffeners. Bracing of the bag was done by adding thin circular sections of polyethylen, connected to the bag at

eight points for each ring. The horizontal placement and circumference of the rings are given in table 3.

Table 3. Placement and size of stiffeners

Ring nr	z-coordinate	Diameter	Circumference
1	-0.15 m	0.72 m	2.28 m
2	-0.30 m	0.64 m	2.02 m
3	-0.45 m	0.48 m	1.49 m

It was assumed that the elasticity modulus of the full scale and model scale stiffeners were equal. For full scale a hollow pipe with diameter $d_p = 18$ cm and thickness $t_p = 1$ cm is intended used. In model scale a circular rod was used, where the scaled diameter of the rod was calculated to 4 mm.

Current and wave experiments were conducted. Current was simulated in the tank by towing the model under the carriage, and the applied waves were regular. Between each run for each filling level, current velocity and wave condition, for both cases, and static deformations of the bag were recorded, by video.

The deformed draft h_d of the bag was estimated based on the image material from camera 1, capturing static deformations for all the experiments. A relationship between the diameter at the free surface and the deformed draft were found, by measuring and comparing distance between pixels in the image. An estimate of the diameter was found based on the difference in x coordinates of point 1 and 2, these points were placed at the edges of the bag at the free surface. An estimate of the draft was found of the mean of the z distances between point 1 and 3, and 2 and 4, point 3 and 4 are placed at the two lowest points of the bag in the image. The placement of the measurement points are illustrated in figure 5. The estimated error of the placement of the coordinates are in the order of ± 5 %.

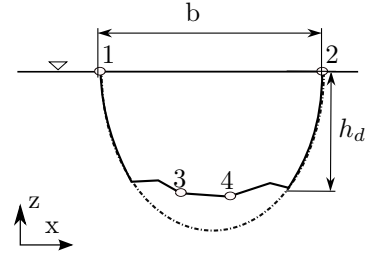


Figure 5. Illustration of marker placement under estimation of deformed draft from images.

The deformed draft h_d was found according to:

$$\frac{D}{h_d} = \frac{x_2 - x_1}{\frac{1}{2}(z_3 + z_4 - z_1 - z_2)}, \quad (4)$$

$$h_d = \frac{D_t}{\frac{D}{h_d}}, \quad (5)$$

where D_t is undeformed theoretical diameter of the full bag.

4. EXPERIMENTAL RESULTS

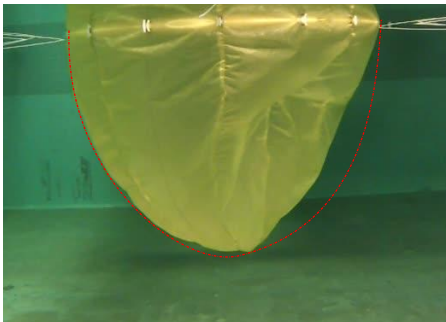
The image material shows a clear tendency that the bag deforms under static pressure when the bag is less than 100% full. These deformations increase in magnitude as expected, with decreasing filling level.

4.1 Static deformation patterns, unrestricted bag

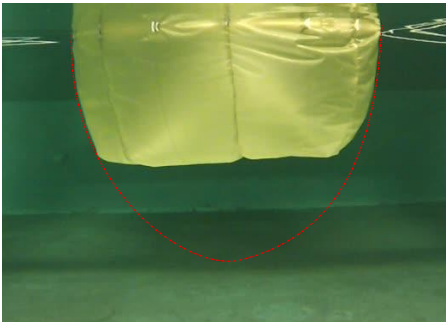
For the normal bag without restrictions, three distinct deformation patterns, from now on referred to as modes of deformation, can be seen from the images. Two symmetric modes (mode 1 and 2), and one unsymmetrical mode (mode 3). These modes appear to be dependent on both filling level and type of loading.

From the current experiments two different patterns can be seen. The deformation modes seem to be directly dependent on the filling level.

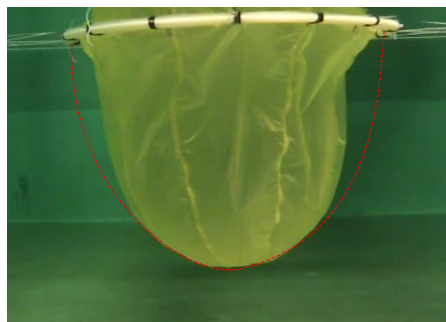
The 90% filling level displays a prevalent trend, an unsymmetrical mode where one of the sides in line with the current is contracted, and the other side remains undeformed, this deformation pattern will be referred to as mode 3. This can be seen from image 6(a), where we clearly see



(a) Current experiments, 90% filling level. Unsymmetrical deformation by contraction of only one side of the bag.



(b) Current experiments, 70% filling. Symmetric deformation by lifting the bottom.



(c) Wave experiments, 70% filling level level. Symmetric deformation by contraction of sides.

Figure 6. Images of static deformation patterns for different filling levels. Undeformed border of 100% full bag indicated by the dotted red lines.

a contraction of the back side of the bag related to the current. Under the experiments it was seen that it was the side opposite to the current, in the deceleration direction that was contracted.

For the 80 % filling level we see a gradual transition from an unsymmetrical deformation similar to figure 6(a) to a symmetric deformation as displayed in figure 6(b), where the bottom is lifted.

For filling levels below 70%, the trend of the deformations does again appear prevalent. The bag now displays a symmetric mode, where the bottom is lifted. This deformation pattern will be referred to as mode 1. This can be seen in figure 6(b).

For the wave experiments a new deformation pattern is observed where the bag now displays a symmetric contraction of the sides. This deformation pattern will be referred to as mode 2. From observation of figure 6(c) we can see that no change in draft can be observed related to the full shape of the bag.

The estimated deformed draft h_d is plotted for all the experiments in figure 10(a). The data can be divided into two distinct categories, one for current and one for the wave experiments. The data of the current experiments indicate a decrease in draft for decreasing filling level that appear linear.

The variance of h_d for the 70 and 80 % filling levels are larger than the remaining experimental series, this was expected for the 80% filling level, as a gradual transition between two different deformation modes were observed. For the 70% filling level the variance can be explained by variance and accuracy between the experimental series.

4.2 Static deformation patterns, braced bag.

For the braced bag only one mode of deformation remains, which is a version of the first mode. The deformation now appear independently of both filling level and type of loading.

It appears that for the braced bag the second and third modes of deformation are restricted from appearing, leaving only a version of the first mode. Figure 7 shows the deformation of the bag for 70% filling level for the current and wave experiments, it can be observed from the figure that the bottom is now lifted for both the cases, contrary to the experience with the unbraced bag.

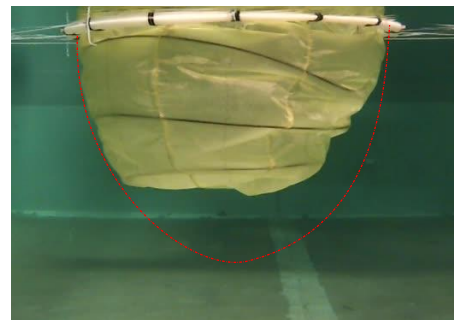


Figure 7. Static deformation patterns of braced bag for 70% filling level, current and wave. Undeformed border of 100% full bag indicated by the dotted red line.

The estimated deformed draft h_d is plotted for all the experiments for the braced bag in figure 10(b). For the braced bag all the data indicate a decrease in draft as the filling level decreases.

Due to the nature of the measurement technique and calculations of the draft estimates, an uncertainty of approximately $\pm 10\%$ is assumed. Despite the errors in the measurement technique, both figure 7 and figure 10(b) indicate that there is a pronounced uniform decrease in draft for decreasing filling levels when bracing is applied to the bag.

5. MODELLING OF STATIC DEFORMATIONS ON BAG FOR DIFFERENT FILLING LEVELS

From analysis of the model experiments, multiple deformation patterns were found. For the unrestricted bag two different symmetric prevalent modes of deformations were found for low filling levels, as shown in figure 6(b) and 6(c). However for the braced bag, a consistent deformation, where the bottom was lifted, were found.

The knowledge that the bag will consequently deform by lifting the bottom when braces are applied, can be used to detect leakages at an early point. This can be done by measuring the pressure at the center at the bottom of the bag, the pressure will decrease if the filling decreases, as the bottom lifts. A significant drop in pressure would indicate a leakage in the bag.

To better understand the responses of both the unrestricted and the braced bag, a model of both the first two deformation patterns is needed.

To assure conservation of mass inside the bag, (3) is used under the modelling of the deformations. However, for simplicity, it is assumed that the volume can be represented in 2D by the deformed area, given and represented in polar coordinates as:

$$A_d = \frac{1}{2}\pi ah\lambda = \int_0^\pi \frac{1}{2}r_d^2 d\theta, \quad (6)$$

where r_d is the radius of the deformed bag in polar coordinates.

The full bag in 2D is represented by the theoretic half ellipse, given in polar coordinates as:

$$r_t(\theta) = \frac{ah}{\sqrt{(h \cos \theta)^2 + (a \sin \theta)^2}}, \quad 0 \leq \theta \leq \pi \quad (7)$$

where $a = \frac{D}{2}$.

The shape of the deformed bag for 70% filling level for the two modes shown in figure 6(b) and 6(c) were captured with image analysis in Matlab. The shapes composed of 25 points, were transferred to a real world coordinate system in polar coordinates, and named r_{dm} , where subscripts m denotes measured. The measured deformations are plotted together with the theoretic ellipse and the deformation model in figure 8.

Instead of modelling the deformed shape directly, the difference between the theoretic ellipse and the deformed shape $r_t(\theta) - r_{dm} = dr_m$, was plotted and modelled. The model of the deformation is than given as:

$$r_d = r_t(\theta) - dr_M(\theta, \lambda), \quad (8)$$

where subscript M denotes modelled.

It is demanded that the model holds for all filling levels, such that:

$$r_d\left(\frac{\pi}{2}, 0\right) = 0, \quad r_d\left(\frac{\pi}{2}, 100\right) = h. \quad (9)$$

A proposed model for the deformation difference, for both the modes are given as:

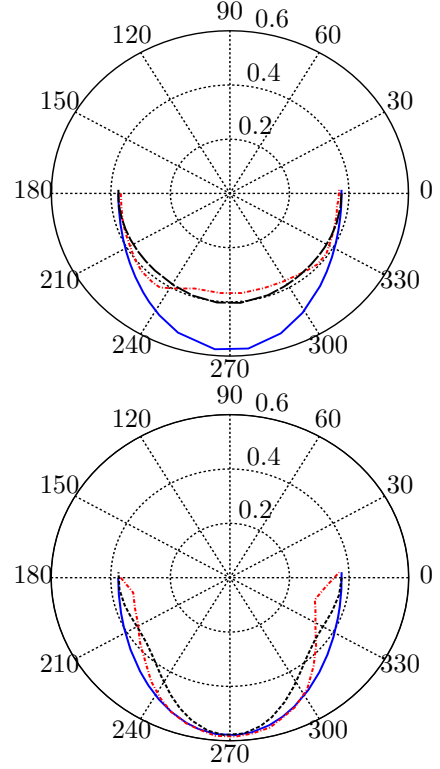


Figure 8. Static deformation patterns. Blue line is the theoretic ellipse, the dotted black line is the measured deformed shape and the red dotted line is the modelled deformed shape. Mode 1 top, Mode 2 bottom.

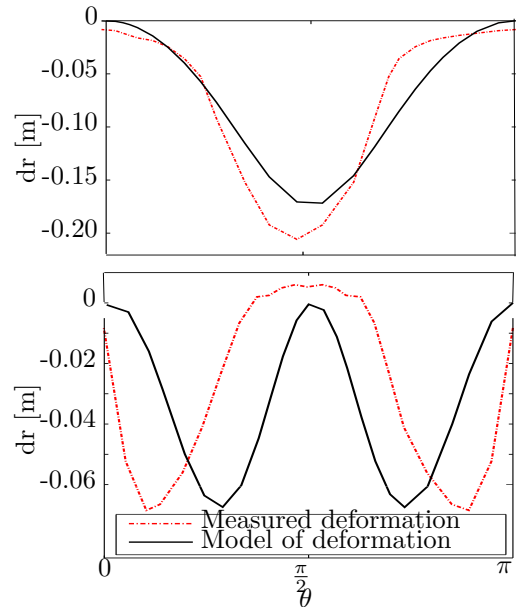


Figure 9. Difference between theoretic shape and deformed shape. Mode 1 topp, mode 2 bottom.

$$dr_{mn}(\theta, \lambda, n) = r_t(\theta) \frac{1}{2n} \left(1 - \frac{\lambda}{100} \right) \left(1 - \sin \left(2n\theta + \frac{\pi}{2} \right) \right), \quad (10)$$

where n is the mode number, giving $n=1$ for mode 1 and $n=2$ for mode 2. The model dr_M is compared to dr_m in figure 8, dr_M is given by the black line and dr_m is given by the dotted red line. Applying (10) in (8) yields:

$$r_d(\theta, \lambda, n) = r_t(\theta) \left(1 - \frac{1}{200n} (100 - \lambda) \left(1 - \sin \left(2n\theta + \frac{\pi}{2} \right) \right) \right) \quad (11)$$

The areas of the measured and the modelled deformed bag is compared to the theoretic deformed area by (6). The error between the areas is computed by $\epsilon_{di} = \frac{|A_d - A_{di}|}{A_d}$, the areas and errors are presented in table 4.

Table 4. Deformed area, and error of modelled and deformed area

Mode nr	λ	A_d	A_{dm}	A_{dM}	ϵ_{dm}	ϵ_{dM}
1	70	0.239	0.230	0.235	0.036	0.019
2	70	0.239	0.311	0.300	0.297	0.253

Both the calculated area from the measurements and the model of deformation mode 1 shows good agreement with the theoretic deformed area. The area of the deformed shape of mode 2 displays much larger errors, this is most probably due to that this deformation is a deformation of the radius, and therefore 3D, resulting in that the assumption of a 2D area is incorrect.

The deformed draft h_d of the two deformation patterns, dependent of the filling is calculated to be:

$$h_{d1} = r_d \left(\frac{\pi}{2}, \lambda, 1 \right) = h \frac{\lambda}{100} \quad (12)$$

$$h_{d2} = r_d \left(\frac{\pi}{2}, \lambda, 2 \right) = h \quad (13)$$

Comparing the model to the measured drafts in the experiments in figure 10, we observe that the model, despite its simplicity, capture the trend. For the unrestricted bag we observe that the mean of the deformations of both the two modes are captured, while for the braced bag the model work as a lower limit for the draft.

6. CONCLUSION

Static deformations of a CFC for different filling levels have been experimentally studied. The image material showed a clear tendency that the bag deforms under static pressure when the bag is less than 100% full. These deformations increase in magnitude, with decreasing filling level. Multiple deformation patterns were found, dependent on filling level and previously applied load. For the braced bag only one deformation pattern was found. A model for a filling-level-dependent deformed draft is presented, and a method for leakage detection have been proposed.

7. ACKNOWLEDGEMENTS

This work have been financed by the research project "External Sea Loads and Internal Hydraulics of Closed Flexible Cages" a knowledge-building project for the aquaculture business sector, in cooperation with SINTEF Fisheries and Aquaculture, industry partners, NTNU, and the Norwegian Research Council. The project is also associated with the Centre for Autonomous Marine Operations and Systems (AMOS)

REFERENCES

- G. Løland and J.V. Aarsnes. Fabric as construction material for marine applications. In *Hydroelasticity in marine technology*, pages 275 – 286, 1994.
- T Rosten, B. F. Terjesen, Y. Ulgenes, K. Henriksen, E. Biering, and U. Winther. Lukkede oppdrettsanlegg i sjø- økt kunnskap er nødvendig. *Vann*, (1), 2013.
- A. Shaw and D. Roy. Improved procedures for static and dynamic analyses of wrinkled membranes. *Journal of Applied Mechanics*, 74(3):590 –594, 2007.
- I.M. Strand, A.J. Sørensen, P. Lader, and Z Volent. Modelling of drag forces on a closed flexible fish cage. In *submitted to 9th IFAC Conference on Control Applications in Marine Systems*, 2013.
- P.T. Sumesh and R. Govindarajan. The possible equilibrium shapes of static pendant drops. *Journal of Chemical Physics*, 133(14), 2010.

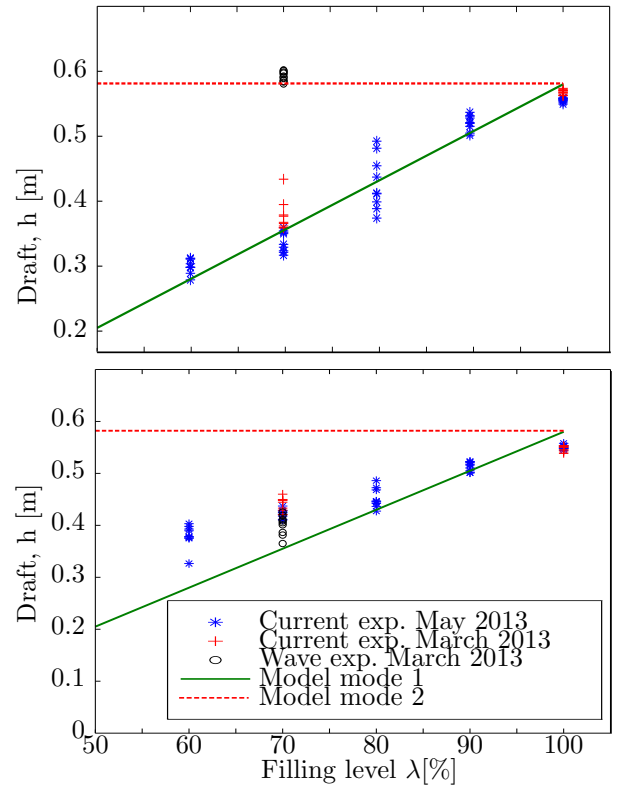


Figure 10. Draft measurements of deformed bag for different filling levels from images taken under the experiments, compared with modelled draft. Unrestricted bag top, restricted bag bottom.

